ACES Asian Chemical Editorial Society

doi.org/10.1002/cnma.202100396

CHEMNANOMAT
Review

www.chemnanomat.org

Nanospace Engineering of Metal-Organic Frameworks for Heterogeneous Catalysis

Qi Wang,*[a] Guoxiang Yang,[a] Yangjie Fu,[a] Ningyi Li,[a] Derek Hao,[c] and Shengqian Ma*[b]

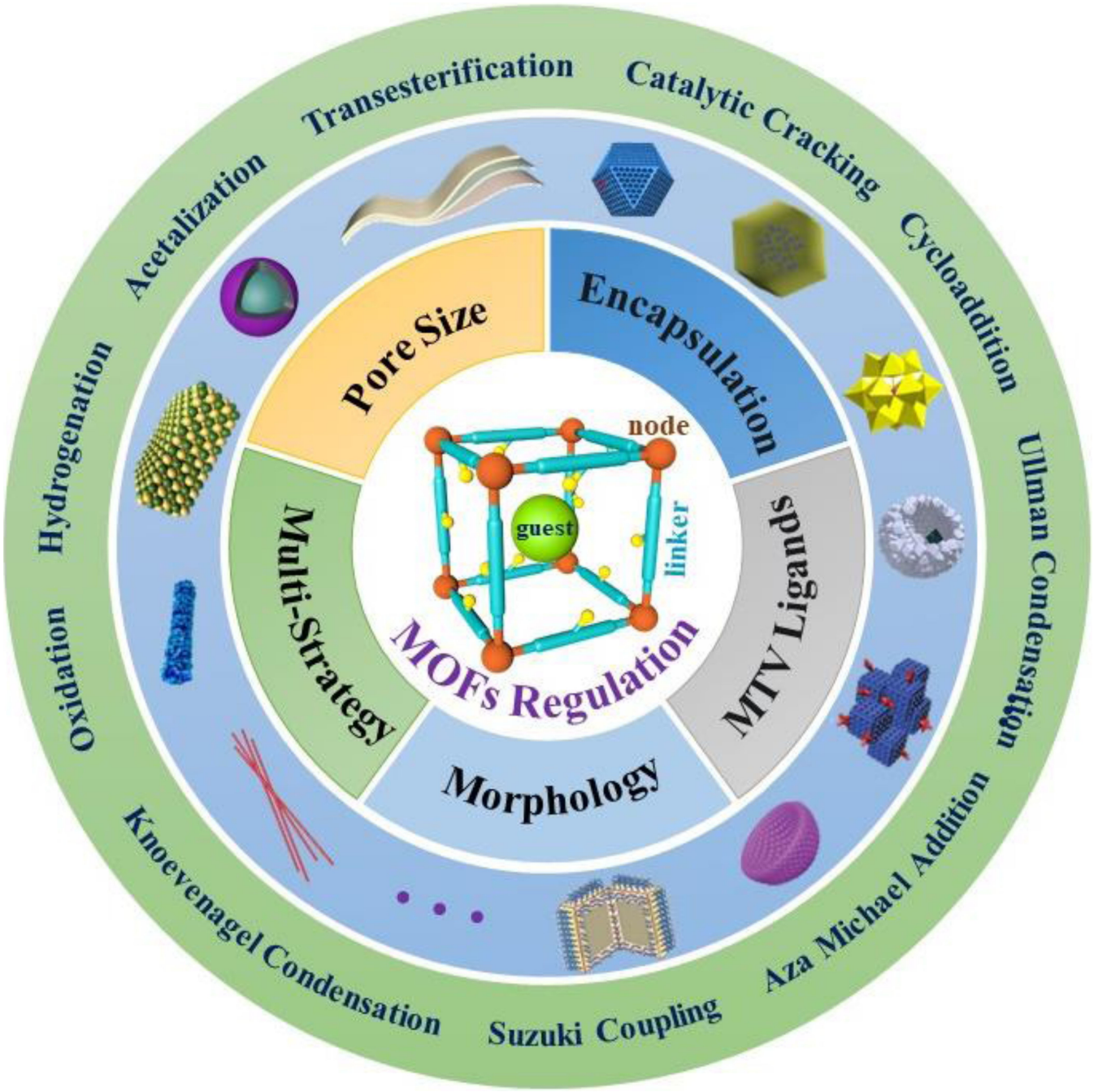

Abstract: The structural advantages of metal-organic frameworks (MOFs) can facilitate wide applications in the field of catalysis, including oxidation, hydrogenation, acetalization, transesterification, catalytic cracking, and so on. The efficiency of catalysis is closely related to the synergy between active center, auxiliary center, and microenvironment. Researchers can customize MOFs according to the needs of catalytic reactions, and many strategies were established for boosting catalytic performance. In this review, we aim to summarize and illustrate recent progress in the nanospace engineering of MOFs. Generally, MOFs were engineered mainly from the following aspects: 1) Regulation of pore size, including micropores, mesopores, and macropores. 2) Engineering of encapsulated active species, such as metal nanoparticles, quantum dots, polyoxometalates, enzymes, etc. 3) Engineering of MOFs morphology from zero dimension to three-dimension. 4) Controllable integration of MOFs with multi-strategies. 5) Construction of multivariate MOFs via introducing multiple or mixed organic functional groups into the existing framework. Besides, for further low cost and practical applications, challenges for MOFs as green and sustainable catalysts are also discussed.

1. Introduction

1.1. Merits of MOFs

Metal-organic frameworks (MOFs) are porous crystalline materials with periodic structures. Herein, metal ions or metal ion clusters are used as nodes, and organic ligands such as aromatic and their derivatives or nitrogen heterocyclic compounds are used as linkers. Through coordination bonds and other weak modes between metal nodes and organic linkers, they are self-assembled to form MOFs. Early in 1995, Yaghi and Li synthesized $Cu(4,4'\text{-bpy})_{1.5}\cdot NO_3(H_2O)_{1.25}$ (bpy: 4,4′-bipyridine) metal-ligand coordination by hydrothermal method and named this kind of material as MOFs.[1] Since then, the research on MOFs has become a hot spot, and tens of thousands of MOFs have been designed and synthesized. According to different synthesis methods and component units, they can be divided into the following categories: (1) isoreticular metal-organic frameworks (IRMOFs), (2) zeolitic imidazolate frameworks (ZIFs), (3) metarial sofistitute Lavoisierframeworks (MILs) and (4) Socket-channel frameworks (PCNs).

Due to the advantages of large specific surface area, high porosity, unsaturated metal coordination sites, diverse structures and functions, extensive use of MOFs were found in gas separation, catalysis, adsorption, biomedicine, sensing, etc. Especially for catalysis, MOFs have triggered great research progress in this field in the past two decades, displaying outstanding performance.[2–4] Thanks to but not limited to the charming porosity, diversity, and flexibility, MOFs have surpassed traditional homogeneous and heterogeneous catalysts in many aspects.[5] It combines the functional characteristics of organic linkers and metal nodes, which are suitable for a variety of catalytic reactions. Till now, MOFs-related materials have been widely applied in various catalytic reactions,[6,7] such as oxidation, hydrogenation, acetalization, transesterification, catalytic cracking, cycloaddition, Knoevenagel condensation, Suzuki coupling, Aza Michael addition, Ullman condensation, etc. Recently, there are also some closely related reviews on MOFs for catalysis.[8–10] For example, Jiang et al. summarized the recent progress of MOF-based materials, such as pristine MOFs, MOF composites, and MOF derivatives were used as heterogeneous catalysis, photocatalysis, and electrocatalysis. Compared with traditional catalysts, they also clearly indicated that the MOF-based materials had significant strengths and weaknesses.[8] Furthermore, to improve the practical ability of MOFs, Xu et al. summarized the recently controllable integration of MOFs and functional materials, which could enhance the MOFs framework stability and catalytic activity. This review mainly introduced the preparation and heterogenous catalytic application of MOFs composites/hybrids.[10]

1.2. Principles of MOF catalysis

Catalysis is crucial in many aspects of modern industrial society. Nowadays, more than 95% of all chemical products (by volume) are produced via catalytic ways, so the study of highly active catalytic materials is exciting and dynamic work. The regulation of the catalytic center microenvironment at the molecular level is the major challenge for traditional heterogeneous catalysts. Whereas, it is much easier to break through this bottleneck in the system of MOFs. As catalysts, MOFs materials can be used as catalytic active centers in three positions, including central ions, organic ligands and structural pores (Figure 1). The unsaturated coordination site of the central metal ions can be used as the active center for catalytic reactions. The functional group existing in organic ligands can also be directly used as the active center, or a new activity center can be formed after post-synthetic modification. Moreover, the structural pores of MOFs can be used as the place or carrier for special catalytic reactions. Active species can be loaded onto the surface or into the pores of MOFs via physicochemical methods such as

[a] *Prof. Q. Wang, Dr. G. Yang, Y. Fu, N. Li*
School of Environmental Science and Engineering
Zhejiang Gongshang University,
Hangzhou 310018 (P. R. China)
E-mail: wangqi8327@zjgsu.edu.cn

[b] *Prof. S. Ma*
Department of Chemistry
University of North Texas
1508 W Mulberry St, Denton, TX 76201 (USA)
E-mail: Shengqian.Ma@unt.edu

[c] *Dr. D. Hao*
School of Civil and Environmental Engineering
University of Technology Sydney (UTS)
Ultimo, NSW 2007 (Australia)

adsorption, impregnation and precipitation so that the reaction eventually takes place on the surface or in the cavity of MOFs.

It is reported that the specific surface area of MOFs can be near or above 7000 m^2/g,[11] which is much higher than traditional porous materials, including zeolite, molecular sieve, and carbon materials. Such porous structures can provide high-density active centers and huge reaction space for catalytic reactions. In addition, MOFs materials have strong interaction between metallic nodes and organic linkers, resulting in stable coordination bonds and a sufficiently rigid porous framework. Therefore, the entry and exit of guest molecules can be ensured without changing the porous structure. Based on this principle, MOFs catalysts can be recycled many times. Moreover, a multifunctional platform has been established based on MOFs for the design of heterogeneous catalysts. The pore size, crystal shape and spatial dimension of MOFs can be accurately controlled by selecting the connection mode between organic ligands and metal central ions. Researchers can customize MOFs according to the needs of catalytic reaction, to achieve the best catalytic effect. In addition, the efficiency of the catalyst is closely related to the synergy between active center, auxiliary center and microenvironment. The controllable integration of MOFs and functional materials can make each component work together and realize collaborative catalysis, to greatly promote the efficiency and stability of MOF-based catalysts.

Qi Wang obtained her B.S. degree (2004) from Wuhan University, China, and graduated from Institute of Chemistry, Chinese Academy of Science with a Ph.D. degree in 2009 under the supervision of Prof. Jincai Zhao. She is currently a professor in the School of Environmental Science and Engineering at Zhejiang Gongshang University. Her research interests focus on photocatalysis, photoelectrocatalysis and environmental catalysis.

Guoxiang Yang received his master's degree (2018) from Shanghai Normal University, China. He obtained his Ph.D. degree (2021) from Osaka University, Japan. Currently, he is a lecturer in the School of Environmental and Engineering at Zhejiang Gongshang University. His research focuses on the design and synthesis of yolk-shell or core-shell materials, and their applications in photocatalytic and environmental fields.

Yangjie Fu received his bachelor's degree (2019) in Environmental Engineering from Zhejiang University of Technology, China. He is currently pursuing his master degree in Environmental Science and Engineering at Zhejiang Gongshang University, China. His research focuses on the design and synthesis of MOFs-based heterojunction and their applications in photocatalytic and environmental fields.

Ningyi Li received his bachelor's degree (2019) in Environmental Science from Henan Institute of Science and Technology, China. He is currently pursuing his master degree in Environmental Science and Engineering at Zhejiang Gongshang University, China. His main research interests are the design and synthesis of environmental functional materials and their applications in the photocatalytic and environmental health fields.

Derek Hao received his bachelor's degree (2017) in materials chemistry from China University of Geosciences, China. He finished his Ph.D. (2021) at Centre for Technology in Water and Wastewater (CTWW), University of Technology Sydney (UTS). Currently, he is a Research Fellow at Centre for Catalysis and Clean Energy, Griffith University. His research interests include the synthesis and application of nanomaterials in energy and environmental areas.

Shengqian Ma obtained his B.S. degree (2003) from Jilin University, China, and graduated from Miami University (Ohio) with a Ph.D. degree in 2008. After finishing two-year Director's Postdoctoral Fellowship at Argonne National Laboratory, he joined the Department of Chemistry at the University of South Florida (USF) as an Associate Professor in 2010, and was promoted to Associate Professor with early tenure in 2015 and to Full Professor in 2018. In August 2020, he moved to the Department of Chemistry at University of North Texas as the Robert A. Welch Chair in Chemistry. His research interest focuses on the development of functional porous materials including MOFs, covalent organic frameworks (COFs), and porous organic polymers (POPs) for energy, biology, and environment-related applications.

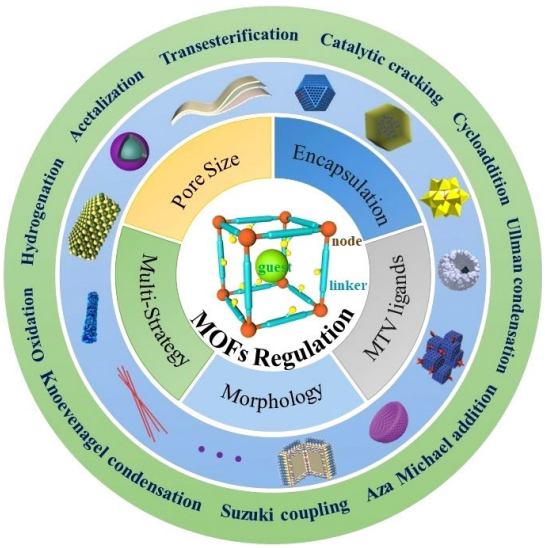

Figure 1. Schematic diagram of MOFs structure, regulation strategies, and their catalytic applications.

1.3. Strategies for boosting performance

To meet the practical applications, many strategies were established to enhance the catalytic performance of MOFs (Figure 1). Generally, MOFs were engineered mainly from the following aspects: 1) Regulation of pore size, including micropores, mesopores, and macropores. 2) Engineering of encapsulated active species, such as quantum dots (QDs), metal nanoparticles (MNPs), polyoxometalates (POMs), molecular species, enzymes, silica, polymers, etc. The activity, as well as skeleton stability, can both be enhanced. 3) Engineering of MOFs morphology from zero dimension (0D) to three-dimension (3D), such as 0D NPs, 1D nanowires and nanotubes, 2D nanosheets, 3D microcapsules and hierarchical nanostructures. Besides, controllable integration of MOFs with multi-Strategies was also proved to be a highly efficient way. The catalytic activity, selectivity and stability in various chemical reactions can be significantly regulated due to synergistic effect.

2. Regulation of pore size

Most MOFs belong to microporous materials. Although it is conducive to the adsorption and separation of small molecules, it also limits the rapid diffusion of molecules and prevents macromolecules from contacting the active sites through micropores. Therefore, the regulation of MOFs channels is conducive to its application in separation and catalysis. It is very important to design and construct MOFs that can achieve the target function and have appropriate pore structure and pore size distribution. Recently, the different catalytic abilities of MOFs with different pore sizes have been reported. As Sun et al. reported a novel water-stable MOF Zn(Py)(Atz) as a heterogeneous catalyst with microporous and outstanding stability for chemical conversion of CO_2 with various epoxides under mild conditions.[12] Zhou et al. designed and synthesized a mesoporous MOF termed PCN-808, based on Zr_6 clusters and tetratomic carboxylate ligands through linker installation. A linear ruthenium-based metalloligand was successfully and precisely installed into the mesoporous PCN-808 MOFs named PCN-808-BDBR. Thanks to the mesoporous nature of the framework of PCN-808-BDBR, it exhibited exceptional yields for photocatalytic oxidation of dihydroartemisinic acid to artemisinin.[13] Li et al. reported highly ordered hierarchically microporous MIL-125 with high specific surface area was used as the photocatalyst for atmospheric chemical fixation of CO_2 through CO_2 carbonylative coupling reactions under ultraviolet irradiation.[14] At present, the mainstream pore size regulation methods can be roughly divided into the following ways: in-situ synthesis, post-synthesis modification, interpenetrating regulation, auxiliary synthesis, and competitive ligand regulation. Among them, the first two strategies are most widely used.

2.1. In-situ synthesis

Although the disadvantage of in-situ synthesis is that it is necessary to pay attention to whether the introduced functional groups or other organic ligands will change the chemical state of MOFs precursor solution, thus affecting the formation of MOFs, the advantages of in-situ synthesis strategy are simple synthesis method, easy to control the morphology and aperture size of MOFs advantages, and so on. In-situ synthesis regulation is to adjust the internal structure of MOFs to the required configuration by reasonably selecting metal clusters and ligands. To accurately regulate the structure of porous materials, Yaghi et al. introduced the concept of a network to build an ideal MOFs structure by reasonably selecting secondary structural units (SBUs).[15,16] Keeping the metal clusters unchanged, MOFs with different pore sizes can be obtained by changing the types of organic ligands.[17] This adjustment method is simple and effective, which often does not need to change the synthesis conditions greatly. Therefore, various functional groups can be introduced into MOFs indirectly. At the same time, when the main structure of the ligand remains unchanged, adding some functional groups can change the pore size of MOFs and provide operation sites for the post-modification of MOFs. In addition, changing the type of metal clusters in MOFs will change the spatial arrangement of MOFs, resulting in the change of the topology and aperture of MOFs.[18] Besides, the coordination between metal and carboxylate is a typical reaction for the synthesis of MOFs. A representative example is a metal-terephthalic acid (M-BDC) series MOFs. The framework of M-BDC is supported by a rigid benzene ring. The pore diameter can be adjusted by adjusting the type of metal ions in SBUs. Through pre-design and selection of structural units with appropriate size, the pore diameter of MOFs materials can be accurately controlled.[19]

In general, for MOFs with the same topology, the pore size increases with the increase of ligand occupied space. When the main structure of the ligand remains unchanged, the pore size of MOFs decreases with the increased number as well as

occupied space of functional groups. When the ligand is fixed, changing the metal ions will change the topology of MOFs as well as the pore size of MOFs. The design and control of MOFs framework can realize the functionalization of MOFs and the adjustment of aperture at the same time.[15]

2.2. Post synthetic modification

Although the post-synthetic modification (PSM) method is complex, it has attracted great attention as an effective and flexible method to change the structure and properties of MOFs.[20] This synthesis strategy can introduce functional groups that cannot be retained under traditional synthesis conditions (for example, high temperature or strong acid/base) or functional groups competing with ligand groups into MOFs.[21] The reactants can modify the skeleton of MOFs via reacting with the ligands or metal ions of MOFs without changing their topology. The pre-formed MOFs channels can meet specific needs through PSM, and provide the possibility of fine-tuning the pore size. Due to the functionalization of MOFs skeleton, man properties may change, including pore size, surface morphology, hydrophilicity, hydrophobicity, adsorption, catalytic properties and stability.

For example, Cohen et al.[22] synthesized an amino group functionalized DMOF-1-NH_2 (5.58 Å). This MOF has a similar structure to the original MOFs, and the amino group can provide a reactive site for post-modification. On this basis, they modified the MOFs with linear acetic anhydride to obtain DMOF-1-AM5 with a pore size of 5.35 Å. Using the bridging-crosslinking method, tandem covalent modification of UiO-66-NH_2 was achieved with poly (ethylene glycol) diglycidyl ether and polyvinylamine. The results indicated that the pore size of UiO-66 decreased from 5.36 to 5.00 Å after PSM.[23]

In addition, the development of click chemistry provides a new idea for regulating the pore size of MOFs.[24] Click chemistry usually refers to the 1,3-dipolar cycloaddition reaction between azides and alkynes. For example, Wang et al. fabricated bifunctional Zr-MOFs (UiO-68-N_3/C≡C) with high stability via using two mixed ligands with azido and acetylene groups respectively (Figure 2).[25] The pore size of the modified Zr-MOFs was smaller than that of the unmodified one. This Zr-MOF provides a special platform (~1:1) for the tandem anchoring of bifunctional groups. For the aldol addition of cyclohexanone with 4-nitrobenzaldehyde or 2-naphthalene, Besides, the size-selective effect can be observed in the aldol addition reaction.[25] For the reaction between 4-nitrobenzaldehyde and cyclohexanone, the conversion of 4-nitrobenzaldehyde reached 95% after 60 h reaction. However, the value was only 9% after 7 days for 2-naphthalene with a larger size.

Moreover, due to the unique properties of MOFs in various applications, the introduction of bifunctional or multifunctional into different MOFs cages has attracted great interest. As shown in Figure 3, Ma's research group reported a stepwise PSM process to create bifunctional MOFs with different types of cages and holes through the selective decoration of cages, and successfully controlled the direction of the required reaction.[26]

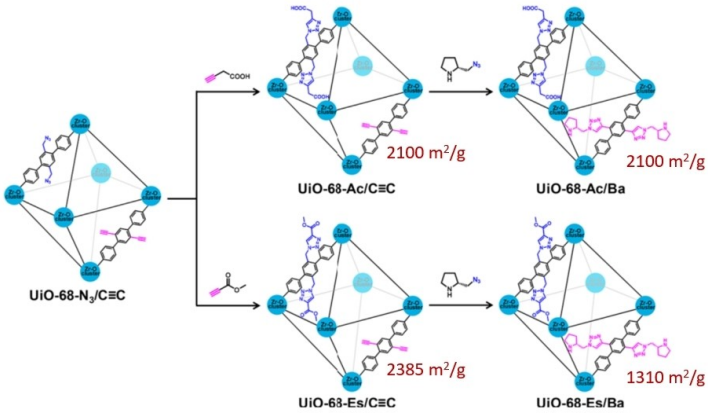

Figure 2. Two PSM routes (-Ac/Ba and –Ec/Ba) for the preparation of modified UiO-68. Reproduced with permission from ACS.[25]

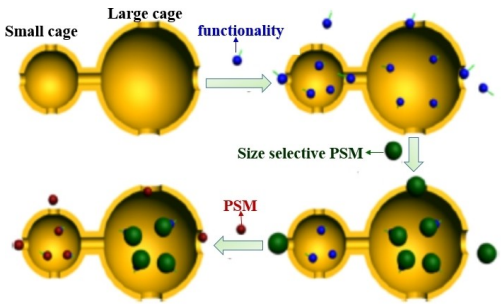

Figure 3. Diagrammatic sketch for the preparation of bifunctional MOFs via stepwise strategy. Reproduced with permission from ACS.[26]

2.3. Interpenetrating regulation

The interpenetration of structures, such as the interpenetration of MOFs frames and the interpenetration between polymer and MOFs frames, can not only improve the stability of MOFs structures but also effectively adjust the pore structure of MOFs.[27] Normally, the mutual insertion of MOFs frames will reduce the aperture, but at the same time, it will improve the stability of MOFs. In addition, some MOFs with interpenetrating structures have unique binding sites/spaces, which can specifically adsorb and separate some components. For example, Zou et al reported two mutually permeable MOFs (SUMOF-2 and SUMOF-3), which were consisted of Zn_4O clusters and dicarboxylate ligands (Figure 4). The structure of SUMOF-2 was similar to that of interpenetrating MOF-5 (8.0 Å). SUMOF-2 was the interpenetrating form of IRMOF-8 (16.1 Å). After mutual penetration through the frame, the pore diameter of SUMOF-2 was reduced to 7.7 Å, and the pore diameter of SUMOF-3 was reduced to 6.6 Å and 9.5 Å.[28]

2.4. Auxiliary synthesis regulation

Changes in reaction conditions lead to different pore sizes of MOFs obtained using the same precursors. The synthesis of

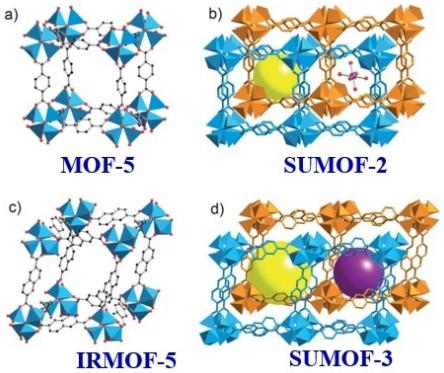

Figure 4. Non interpenetrating model (a, c) and actual crystal structure (b, d) of double interpenetrating frameworks. Reproduced with permission from RSC.[28]

defective MOFs with regulators can increase the pore size, porosity and specific surface area, which finally give special properties. Among them, the most common method is to add a large number of monocarboxylic acids in the process of MOFs synthesis. For example, in the presence of monocarboxylic acid (Figure 5), the metal ions in UiO-66 will preferentially form defective metal clusters with the regulator, which slows down the crystallization rate, resulting in the lack of ligand connection in some regions and the increase of pore size.[29]

Using structure-directing agent (SDA) as a soft template, hierarchical and porous MOFs can be synthesized. Generally, the template occupies a certain space in the hole of MOFs and can be removed by chemical or heat treatment, resulting in a large cavity in the framework of MOFs. For example, Zhang et al. used cetyltrimethylammonium bromide (CTAB) as the structure-directing agent to synthesize HKUST-1.[30] By increasing the initial molar ratio of CTAB to Cu^{2+}, the mesoporous diameter of MOFs increased from 3.8 nm to 5.6 nm. Meanwhile, they also explored the effect of hydrophobic 1,3,5-trimethylbenzene (TMB) as an auxiliary structure-directing agent. The mesoporous size of MOF can be expanded to 31 nm after the incorporation of TMB. Besides, macroporous MOFs can also be observed via template method.[31] 2-methylimidazole and Zn^{2+} as initial precursors of ZIF-8 were first filled into polystyrene ball (PS) forming precursor@PS. ZIF-8 were subsequently grown in CH_3OH-NH_3·H_2O mixture. Finally, the template (PS) was removed and SOM-ZIF-8 was generated with macropore size of 190~470 nm via adjusting the particle size of PS template. The interconnected macropores are beneficial for the accessibility of active sites and the diffusion of macromolecules. In the Knoevenagel reaction of benzaldehyde with malonitrile, SOM-ZIF-8 exhibited higher catalytic activity and recoverability than traditional MOFs.

Moreover, competitive ligands are usually referred to as monodentate ligands with relatively weak deprotonation ability. These ligands can regulate the coordination balance and promote or inhibit crystal growth by competing with polydentate ligands. The nucleation of MOFs can be regulated by changing the concentration of competitive ligands, to form MOFs with various pores and sizes. For example, Wang et al. explored the effect of 2-methylimidazole as a competitive ligand on the pore sizes of MOF-5, HKUST-1, Co-MOF-74, Ni-MOF-74, and NH_2-MIL-101(Fe). Methylimidazole ester, as both a competitive ligand and a base, can accelerate the nucleation of MOFs and produce multistage pores in MOFs. Moreover, the pore size increases with the enhanced concentration of 2-methylimidazole.[32]

3. Engineering of encapsulated active species

The species with specific catalytic sites can be encapsulated in the pores or cages of MOFs. Using the adjustable pore size of MOFs, the entry of effective substances can be engineered and the loss of active substances in the core can be prevented. Combined with the advantages of large elasticity of MOFs shell, ordered crystalline pores and many coordination sites, significantly enhanced catalytic performance can be obtained. In the past decade, controllable preparation of core-shell or core-shell like active species@MOFs composites have attracted great attention, and great progress has been made in this field. So far, many core substances have been selected to be encapsulated in MOFs shell, such as metals, metal oxides, POMS, QDs, MOFs, enzymes, organic ligands etc. According to the contact between core and shell, whether there is a gap between them, it can be divided into core-shell and yolk-shell structures.

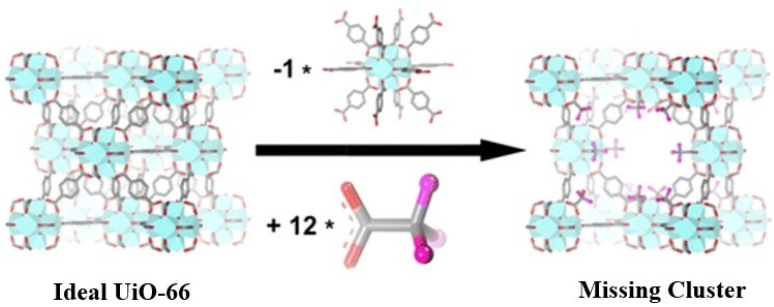

Figure 5. Schematic diagram for the preparation of defective UiO-66. Reproduced with permission from ASC.[29]

3.1. MNPs@MOFs

Using the permanent pores of MOFs to limit guest species, especially metal nanoparticles (MNPs), the catalytic performance can be improved, and the scope of application can also be expanded. Numerous studies indicated that MOFs could limit or stabilize small MNPs with good catalytic activity and recyclability.[33,34] For example, well defined MNPs were encapsulated into MOFs forming core-shell nanostructures. The selectivity, reactivity and durability of the catalyst can be greatly enhanced. Moreover, additional functions could also be provided.[35] Noble MNPs (such as Au, Ag, Pd and Pt) with unique physicochemical and catalytic properties, were most widely studied.[36] Early in 2012, the Huo's group reported a controllable and easy strategy for the encapsulation of adjustable NPs (Pt or Au) within the matrix of ZIF-8.[37] With the assistance of PVP modification and controlled addition sequence, the controllable spatial distribution of nanoparticles can be achieved. For the catalytic hydrogenation of alkenes, the as-prepared Pt@ZIF-8 composite displayed absolute regioselectivity toward n-hexene versus cis-cyclooctene.

Later, for the first time, Xu et al. successfully loaded ultrafine Pt NPs (1.8 ± 0.2 nm) into the cavity (2.9 and 3.4 nm) of MIL-101 via water/n-hexane double solvent method.[38] Since the open windows (1.2 and 1.6 nm) of MIl-101 is slightly smaller than the size of NPs, the loss of Pt can be prevented during the reaction. Especially, the aggregation of Pt NPs on the outer shell can also be avoided by the "double solvent" method. The uniform distribution of Pt NPs in the cavity was confirmed by TEM and electron tomography measurements. The as-prepared Pt@MIL−101 displayed high and stable performance in various heterogeneous catalytic reactions, including ammonia borane dehydrogenation/hydrolysis and CO oxidation. For example, the catalytic hydrolysis of aminoborane can be completed within 2.5 min by Pt@MIL-101 with 2 wt% Pt, which was 2 times faster than the conventional Pt/γ-Al_2O_3 system. Besides, Pd NPs was also encapsulated in ZIF-8.[39] Using $NaBH_4$ as reducing agent, the core-shell Pd@ZIF-8 can efficiently catalyze tetranitrophenol to aminophenol. (Figure 6) The catalytic activity at room temperature is significantly higher than that of traditional ZIF-8 and Pd–C catalysts.

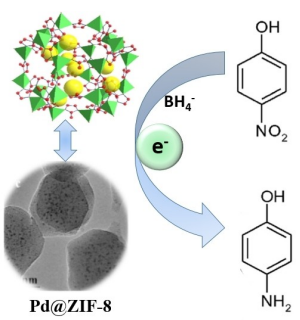

Figure 6. Schematic illustration of Pd@ZIF-8 for *p*-nitrophenol reduction. Reproduced with permission from Elsevier.[39]

In addition to single metal NPs, bimetallic nanoparticles were also encapsulated into MOFs. Especially, bimetallic core-shell NPS has unique properties and great potential in heterogeneous catalysis. For example, Jiang et al. reported that bimetallic nanoparticles with core-shell structure were stably immobilized in ZIF-8 by an easy continuous deposition reduction method.[40] ZIF-8 was firstly desolvated before immersing in aqueous Au and Ag precursors. After reduction and drying, Au@Ag core-shell nanoparticles were obtained on the substrate of MOFs. Compared with Ag or Au single NPs, the special Au@Ag NPs immobilized on MOFs showed a strong bimetallic alloy effect and higher catalytic activity for nitrophenol reduction.

In addition to core-shell structure, the yolk-shell nanostructures have great potential for catalysis, due to their multifunctions composed of nanoparticle cores, microporous shells and cavities.[41–48] The MOFs shell can finely control the selective mass transfer of reactants. Only reactants with molecular $\leq$ pore size are perimitted to diffuse into the cavity. In addition, the large cavity between the yolk and MOFs shell could boost the diffusion of the substrate to the catalytic yolk. For example, Tsung's group developed a general and versatile strategy for preparing Nanocrystal@MOFs with a yolk-shell structure.[42] Herein, Cu_2O was specifically selected as a sacrificial template. Cu_2O can be spontaneously etched due to the production of protons via the formation of ZIF-8. Meanwhile, the clean surface of Cu_2O was beneficial for ZIF-8 coating (Figure 7A). The special Pd@ZIF-8 yolk − shell displayed a size-selective effect toward olefin hydrogenation. Herein, if the molecular size of the substrate is smaller than the pore size of ZIF-8 shell (3.4 Å), it can easily diffuse into the cavity and interact with the Pd core (Figure 7B). On the contrary, large molecules will be blocked outside the shell. Thus, high and negligible performance can be observed for the catalytic hydrogenation of ethylene (2.5 Å) and cyclooctene (5.5 Å), respectively.

In addition, the Au@ZIF-8 yolk-shell was also developed with the assistance of a sacrificial template.[47] As shown in Figure 8A, monodisperse and uniform Au NPs (ca. 15 nm) were first coated by silica. The as-prepared Au@silica was then modified by polyvinylpyrrolidone (PVP), followed by immersing into the growth solution of ZIF-8. The obtained shell (ZIF-8) is extremely stable in alkaline conditions, while silica is unstable. Thus, with the assistance of NaOH, the silica layer can be etched, forming yolk–shell Au@ZIF-8 with large pores. For the selective oxidation of alcohols (with different short-axis sizes), it displayed molecular size selectivity. When the molecular size of substrate is smaller than or matching with the aperture size of ZIF-8 (3.4 Å), the catalytic oxidation can proceed. On the contrary, too larger molecules will be blocked outside, leading to negligible performance. As shown in Figure 8B, the conversion of 1-butanol (short-axis size: 2.9 Å) and 1-hexanol (short-axis size: 3.1 Å) was more than 40%, while the conversion of 3-phenylpropanol (short-axis size: 6.3 Å) was negligible. Meanwhile, the Au@ZIF-8 was also tested as the control sample. It can be observed that the Au@ZIF-8 yolk-shell exhibited significantly boosted catalytic activity. The reason may be attributed to huge cavities in yolk-shell structure, which can

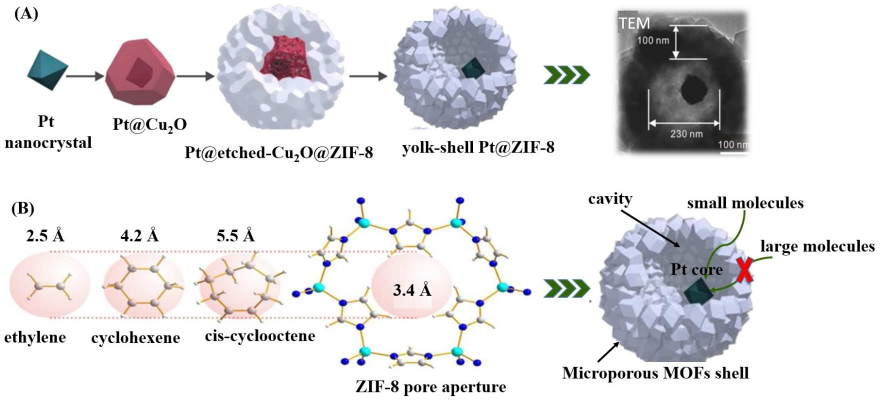

Figure 7. (A) Preparation processes for yolk-shell Pt@ZIF-8 nanostructure, (B) Molecular size induced catalytic hydrogenation of olefin using the optimized yolk-shell structure. Adapted with permission from ACS.[40]

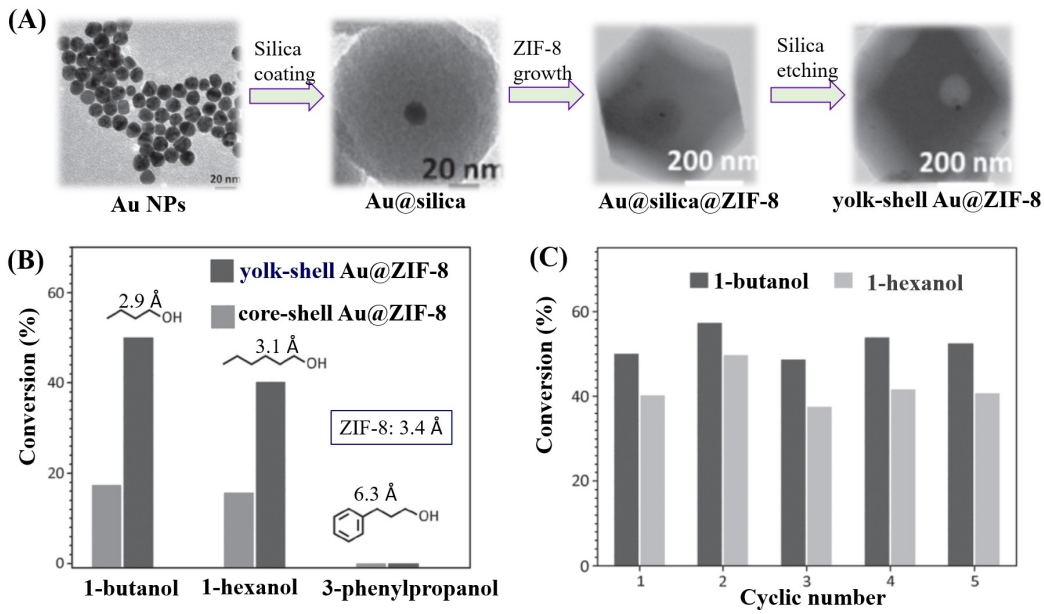

Figure 8. (A) The processes for shape changing of Au@ZIF-8, (B) Catalytic performance for alcohol oxidation by Au@ZIF-8 with different structure, and (C) stability of Au@ZIF-8 yolk-shell in cyclic runs. Adapted with permission from WILEY. [47]

dramatically promote the mass transfer process, and provide ample space to maximize the accessible active sites. Besides, due to encapsulation in the pore of ZIF-8, the aggregation of active Au NPs is not easy to occur. Thus, high catalytic performance can be well maintained in cyclic runs (Figure 8C).

3.2. Metal oxide@MOFs

In addition to MNPs, metal oxide, especially semiconductor photocatalyst was also encapsulated into MOFs. For example, Co_3O_4@MOFs with yolk-shell structure was fabricated by Cai et al (Figure 9A).[49] The composite was used to activate PMS to produce highly oxidizing sulfate radical ($SO_4^{\bullet-}$) for catalytic degradation of p-chlorophenol (4-CP). Compared with core-shell Co_3O_4@MOFs, boosted activity can be observed (Figure 9B). Moreover, the leaching of Co was greatly inhibited due to the presence of MOFs shell. Comparing with bare Co_3O_4 (2.5%), the percentage was ca. 0.28% after 6-h reaction (Figure 9C). Thus, superior stability for 4-CP degradation can be observed for the cyclic runs (Figure 9D). Herein, MOFs have porous and meso-porous structures (pore size 4.2 nm), PMS and 4-CP can enter and exit the surface of the core-shell structure freely and quickly like degradation products (Figure 9E). MOFs can adsorb 4-CP through the π-π bonds, so that 4-CP is enriched in the core-shell structure. Meanwhile, the effective component $KHSO_5$ of PMS can also enter and exit the surface of the core-shell structure, which will subsequently be activated by Co_3O_4 to produce $SO_4^{\bullet-}$. In this way, 4-CP enriched in the core can be oxidized and degraded by $SO_4^{\bullet-}$.

Magnetic Fe_3O_4 particles can also be wrapped into the cavity of MOFs, forming an easy-recyclable catalyst. For

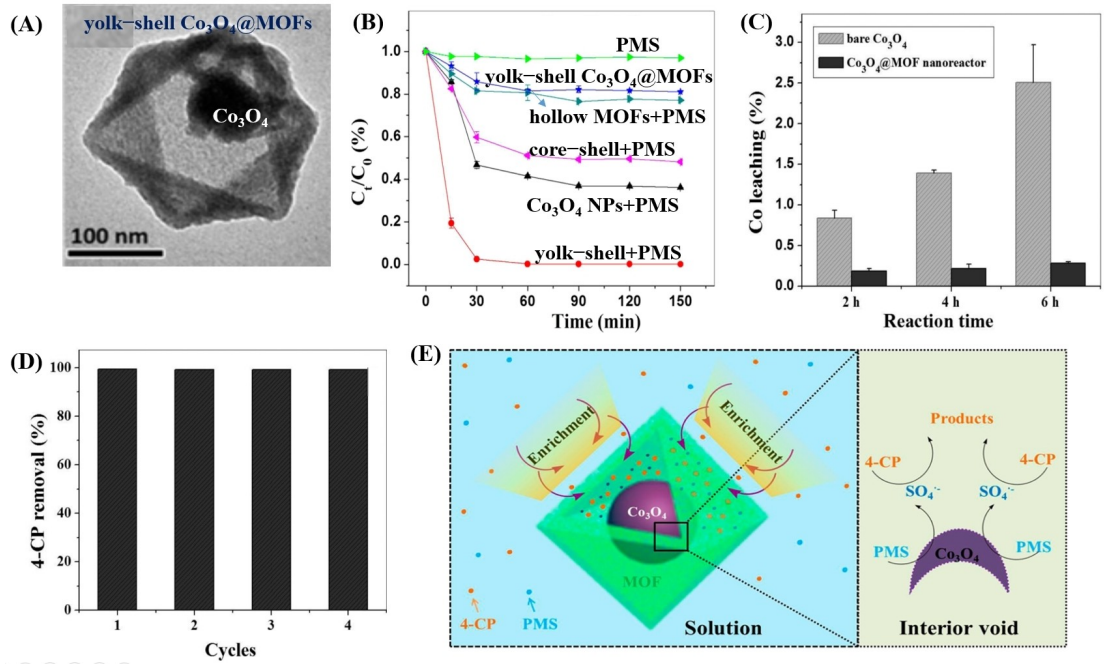

Figure 9. (A) TEM image of yolk-shell Co_3O_4@MOFs, (B) Degradation of 4-CP by different catalysts, (C) leaching of Co in different systems, (D) Cyclic runs of yolk-shell Co_3O_4@MOFs for 4-CP degradation, (E) Proposed mechanism for 4-CP degradation by yolk-shell Co_3O_4@MOFs with PMS. Adapted with permission from ACS.[49]

example, Jiang et al. synthesized Fe_3O_4@MIL-100(Fe) photocatalyst for MB degradation.[50] Under irradiation, electrons (e^-)-holes (h^+) will be generated and separated in the conduction band (CB) and valence band (VB) of MIL-100(Fe), respectively. After light-induced electron transfer to H_2O_2/H_2O, hydroxyl radical (HO·) will be generated, which can oxidize and degrade MB in water. Meanwhile, the photogenerated h^+ also have a strong oxidative ability and can directly oxidize the adsorbed organic molecules.

3.3. POMs@MOFs

Polyoxometalates (POMs) are compounds composed of metals (generally transition metals) and oxygen (Figure 10 A–B). The classic Keggin type POMs is an environment-friendly bifunctional catalyst with strong brönsted acidity and reversible redox activity. However, there are few catalytic active sites exposed on the surface due to too small specific surface area (less than 10 m^2/g). To break through these bottlenecks, POMs molecules were encapsulated into the channels/pores of MOFs forming POM@MOFs composite. It combines the structural character-

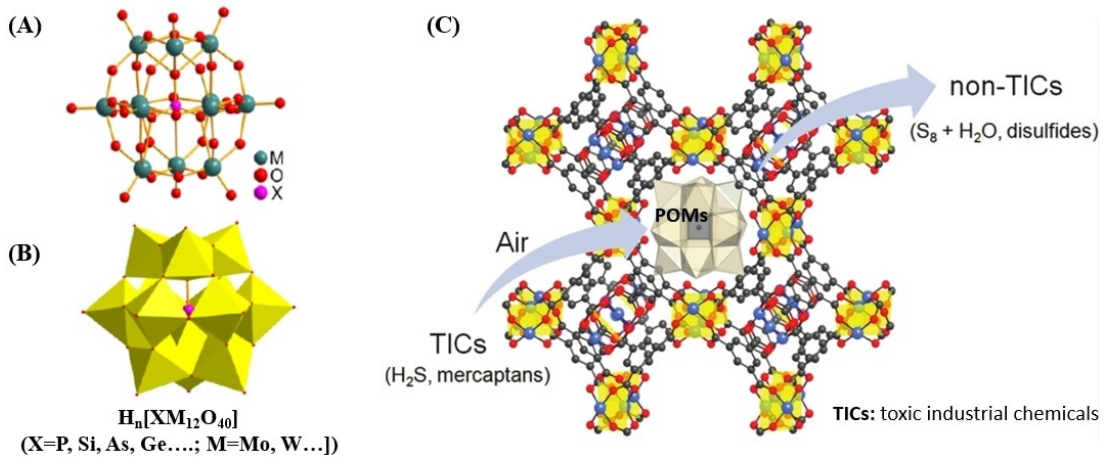

Figure 10. The structure of Keggin-type POMs with ball and stick mode (A) and polyhedron (B), crystal structure of POMs@MOF-199 (C). Reproduced with permission from ACS.[53]

istics and advantages of both POMs and MOFs, including: 1) A variety of catalytic active sites, such as brönsted acid and redox activity sites of POMs, metal or ligand catalytic active sites of MOFs. 2) High dispersion of POMs at molecular level in the channels of MOFs, leading to efficient separation of active sites. 3) The easy transport and selective reaction of substrate molecules due to periodic pore structure of MOFs. 4) Stronger thermal stability and solvent stability.

In 2002, the Keller's research group introduced Keggin type POMs into the 3D framework of Cu-4,4′-bipy (4,4′-bipy = 4,4′-bipyridine) through "one pot" method to obtain the first Keggin type hybrid material $[Cu_3(4,4'\text{-bipy})_5(MeCN)_2][PW_{12}O_{40}]\cdot 2\,C_6H_5CN$.[51] Later in 2005, Margiolaki et al. first introduced the defect Keggin type $K_7PW_{11}O_{39}$ into the framework of MIL-101(Cr) through the post-synthesis method.[52] Hill et al. prepared POMs-based Cu-MOF $[Cu_3(C_9H_3O_6)_2]_4[\{(CH_3)_4N\}_4Cu\ PW_{11}O_{39}H]$ as the oxidation catalyst to realize the oxidation of H_2S to S_8 (Figure 10C).[53] Recently, a novel POMs-based MOF (NENU-500) was fabricated. Due to the redox activity of POMs units and the high porosity of MOF, NENU-500 exhibited excellent electrocatalytic activity for hydrogen evolution.[54] Furthermore, the Farha's group encapsulated $H_3PW_{12}O_{40}$ into mesoporous Zr-MOF (NU-1000) by post immersion method. The as-prepared PW_{12}@NU-1000 composite displayed high porosity and acid/alkali resistance. A series of catalytic studies have been carried out using this composite material. High catalytic activity can be observed toward oxidation of p-sulfide, isomerization and disproportionation of o-xylene.[40,41] The Keggin polyanion $[CoW_{12}O_{40}]^{6-}$ can also be loaded into the pores of ZIF-8. The obtained $H_6CoW_{12}O_{40}$@ZIF can be used as electrocatalysts, showing high activity and cyclic stability for water oxidation.[55]

3.4. GQDs@MOFs

Due to excellent properties, including low toxicity, chemical stability and obvious quantum confinement effect, graphene quantum dots (GQDs, size $\leq$100 nm) are considered a new kind of catalytic material. In 2013, Banerjee et al. embedded GQDs (ca. 5 nm) inside the matrix of MOFs (ZIF) for the first time. Without any capping agents, GQDs can be stabilized inside the pores of ZIF-8. Meanwhile, the shape of ZIF-8 changed from rhombic dodecahedron to spherical with smaller size after encapsulating GQDs.[56] Recently, GQDs were used to fabricate hierarchical micro-mesoporous MIL-101(Cr).[57] The carboxyl-rich GQDs play a vital role as nucleation sites for the growth of defective MIL-101(Cr) (Figure 11). Tiny loading of GQDs (1–4 wt %) can result in steric resistance, structural defects and mesopores in GQDs@MIL-101(Cr). Besides, GQDs were also embedded into the holes of Zn-MOF (Zn-Bim-His). As shown in Figure 12, the as-prepared GQDs@Zn-MOF displayed boosted photocatalytic activity for CO_2 reduction. The production rate was 20.9 $\mu mol\,h^{-1}\,g^{-1}$ for CH_4, of which the selectivity was up to 85%.[58]

3.5. Enzymes@MOFs

Enzyme is a kind of highly selective and efficient natural catalyst, which generally needs to be fixed on the carrier for

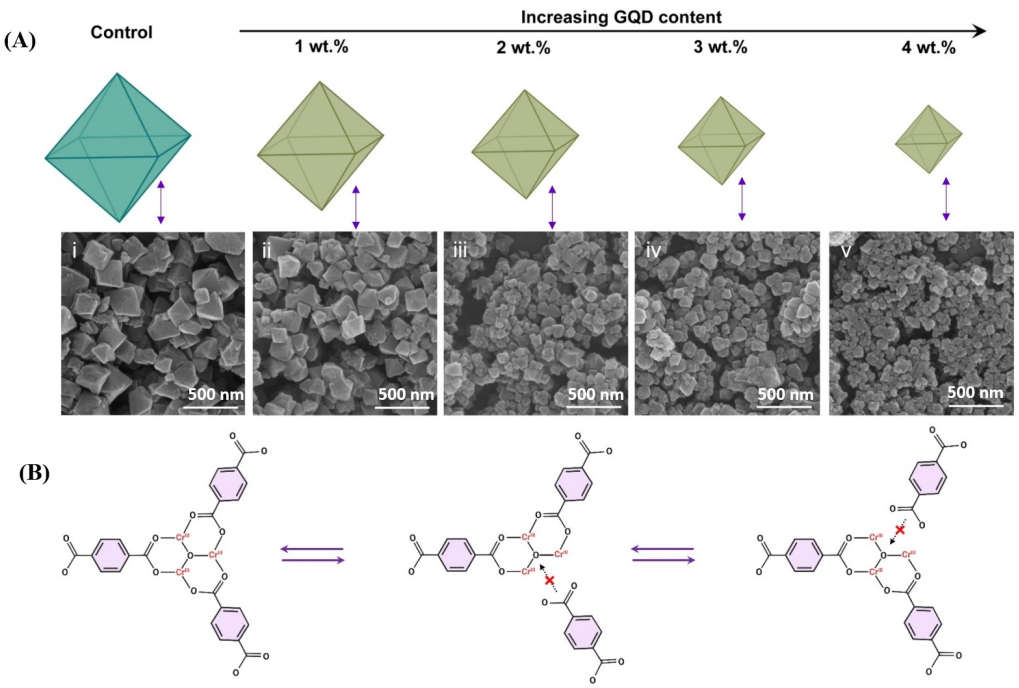

Figure 11. (A) The influence of GQD content on the crystal structure and corresponding SEM images of MIL-101(Cr), (B) Mechanistic illustration for the steric hinderance caused by the presence of GQD. Reproduced with permission from Elsevier.[57]

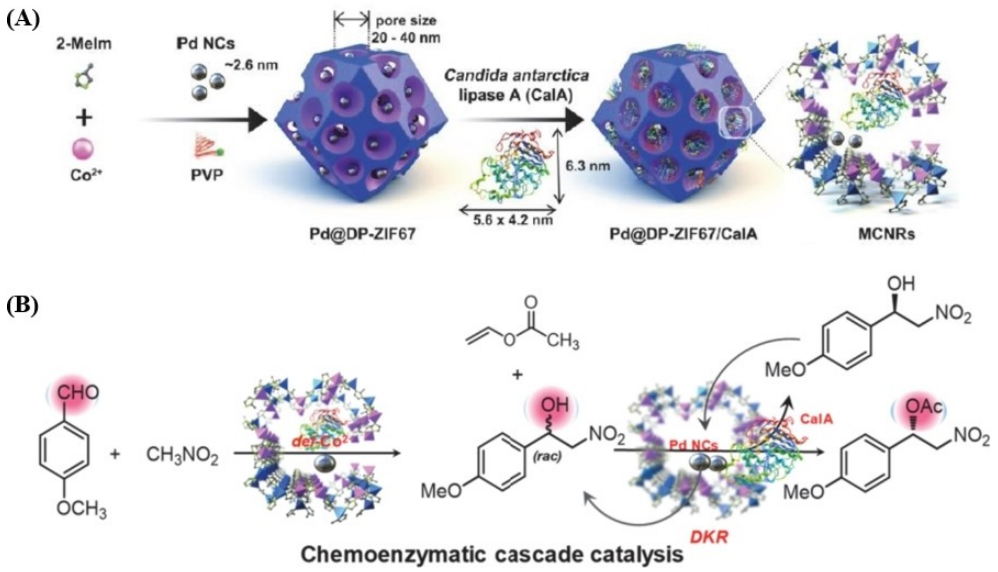

Figure 12. Schematic illustration for (A) the fabrication and (B) catalytic application of Pd@DP-ZIF67/CalA. Reproduced with permission from Wiley.[62]

effective recovery. Enzymes can be introduced into the pores of MOFs forming enzymes@MOFs. The unique physical-chemical properties of MOFs (high porosity and adjustable pore size) and high catalytic activity of enzymes can be combined in the composite. Moreover, the enzyme activity of the composites can be well maintained or even enhanced under denaturing conditions. Therefore, in recent years, the enzymes@MOFs composites have attracted extensive attention.[59–62]

For example, DP-ZIF67 with ultra-large mesopores (20-40 nm) and rich defects were prepared in the presence of polyvinylpyrrolidone (PVP) (Figure 12). The large pores can serve as hosts for ENCAPSULATING guests with smaller sizes, such as MNPs and enzymes.[62] As shown in Figure 13A, Pd NCs were firstly loaded onto ZIF67 forming Pd@DP-ZIF67. Subsequently, Candida antarctica lipase A (CalA) was incubated. For the reaction of p-anisaldehyde with nitromethane, the as-

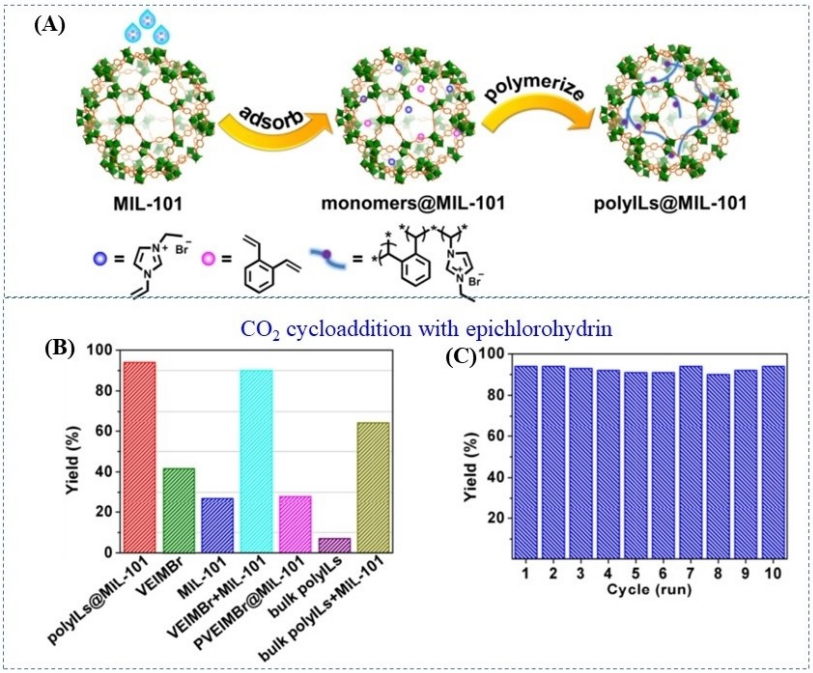

Figure 13. (A) Schematic illustration for the fabrication of polyILs@MIL-101, (B) Catalytic performance by different catalysts, (C) Cyclic performance of polyILs@MIL-101. Adapted with permission from ACS.[65]

prepared Pd@DP-ZIF67/CalA displayed significantly enhanced catalytic activity (Figure 12B). The desired chiral product (acetylated nitroalcohol) can be easily obtained ($>$97% conversion) with high selectivity ($>$99% ee).

3.6. Polymer@MOFs

The nanopores of MOFs can destroy the natural winding of polymer chains and bring new characteristics.[63] For example, polymerization changes dramatically due to constraints at nanochannel scale, and the engineering of the main structure (sequence, tactical or branching) can be easily achieved. Due to restriction and extension of chain, the physical/chemical properties can be greatly improved relative to the bulk ploymers. For example, Huo et al. reported the incorporation of sulfonate polystyrene (PSS) inside the cavity of MIL-101(Cr) via in-situ polymerization. The as-prepared PSS@MIL-101(Cr) was applied as solid acid catalysts for esterification reactions.[64] For the esterification between acetic acid and n-butanol, significantly enhanced catalytic activity (turn over frequency) can be observed due to larger surface area and internal hydrophobicity of MIL-101(Cr). Moreover, these composites exhibit excellent activity and durability in acid-catalyzed reactions. Besides, the Jiang's group also prepared polyILs@MIL-101 via confining imidazolium-based poly(ionic liquid)s (polyILs) into MIL-101(Cr) (Figure 13).[65] The obtained polyILs@MIL-10 displayed excellent CO_2 capture capability as well as catalytic activity. The cycloaddition of CO_2 with epoxides can be efficiently catalyzed to form cyclic carbonates without the addition of any co-catalyst.

3.7. Organic ligands@MOFs

Recently, to design recyclable MOFs catalysts and to improve the efficiency of catalysis, there are many reports about constructing functionalizing MOFs with organic ligands via a post-synthetic installation strategy.[66,67] For example, Zhou et al. reported Bronsted acid sites were encapsulated into porphyrinic MOFs (PCN-222-SO_4) with large channels, high surface areas, and tailored pore environments through a post-synthetic installation method.[66] The PCN-222-SO_4 as a dual-functional solid acid/photocatalyst can be used for the tandem semisynthesis of artemisinin. Thanks to the tailored pore environment and enhanced cooperativity within one channel during catalytic conversion, the PCN-222-SO_4 displayed enhanced selectivity, recyclability, and stability. This result highlights the synergistic advantages of MOFs catalysts coated with homogeneous organic ligands, enhancing the catalytic performance and improving its stability.

4. Engineering of morphology

A large number of studies indicate that the size and morphology of MOFs have a great impact on catalytic reactions. Therefore, the regulation of morphology (including size and shape) of MOFs has gradually become one of the research hotspots. So far, 0D to 3D MOFs have been gradually synthesized and reported.[68–71] For example, 0D and 1D nano MOFs are mainly synthesized by the following three methods: 1) Controlling the formation and self-assembly of MOFs on the nanoscale with emulsifier or template. 2) In the early stage of MOFs formation, MOFs were precipitated rapidly by introducing poor solvent, microwave heating or ultrasonication. 3) Regulators were added in the process of synthesizing to regulate the size and morphology. The 3D MOFs also can be regulated by the above three kinds of regulation methods. However, the self-assembly of MOFs materials in 3D space is much more complex. 3D MOFs are usually prepared by hard/soft template method, liquid-liquid and gas-liquid interface reaction, etc.

4.1. Nanoparticles

Nano microemulsion is a suspension consisting of many small droplets. It can be used as a "nanoreactor" to restrict the nucleation, growth and self-assembly processes of MOFs due to the special structure of oil-in-water or water-in-oil. In this method, metal and organic ligands are usually dissolved in water and oil phases, respectively. They were further separated by surfactants on the surface of droplets. When droplets collide or the solution is stimulated by external stimuli, such as temperature change, light and microwave radiation, droplets will break or polymerize, so that metal and ligands meet to form MOFs. The whole process takes place in droplets, so the particle size of MOFs prepared by this method is generally small. For example, Mann et al. successfully prepared Prussian blue NPs in the oil-in-water nano-emulsion with a particle size as low as 12 nm.[72]

Besides, grafting polymers onto the surface of MOFs can also lead to well-dispersed MOF NPs. For example, Webley et al. synthesized poly MOF material (P@MOF) with UiO-66-NH_2.[73] As shown in Figure 14, once the same amount of UiO-66-NH_2 and P@MOF were dispersed in water, UiO-66-NH_2 particles gather easily and cannot be dispersed by ultrasound (left), while P@MOF (20–70 nm) can be evenly dispersed in water in the form of small particles due to the existence of polymer. For the selective catalytic reduction of 4-nitrophenol (NP), conversion

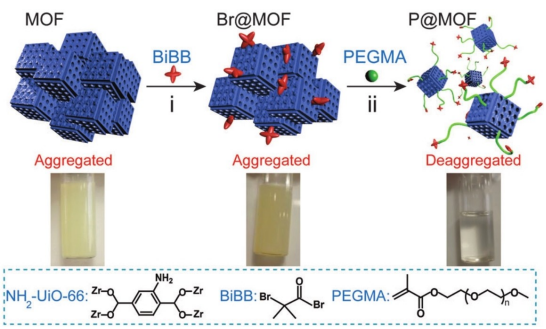

Figure 14. Schematic processes for the preparation of P@MOF. Reproduced with permission from Royal Society of Chemistry.[73]

frequency (TOF) was 2.26 and 7.98 $h^{-[1]}$ by Pd/UiO-66-NH_2 and Pd/P@MOF, respectively. The value was greatly enhanced by 2.5 times due to the presence of well-dispersed P@MOF.

4.2. Nanowires

Template-assisted epitaxial growth method was applied to grow MOFs on Co_3O_4 nanowire arrays. As shown in Figure 15A, the as-prepared Co_3O_4@MOF-74 displayed a core-shell structure.[74] By controlling the number of solvothermal cycles, the thickness of MOFs shell can be adjusted freely in a wide range. Compared with pure Co_3O_4 nanowires, the core-shell Co_3O_4@MOF-74 displayed significantly enhanced catalytic performance for oxygen evolution reaction (OER) (Figure 15B). As for optimized Co_3O_4@MOF-74, it can produce a large current density (50 mA/cm^2) and small Tafel slope at very low overpotential (285 mV). It is further found that MOF-74 was converted to cobalt hydroxide, which plays a role as a practical catalytic center in electrocatalytic oxygen production. This work not only provides a new method for preparing core-shell MOFs, but also reveals the in-situ conversion mechanism of MOFs-based materials in the electrochemical reaction, which provides a valuable reference for the development of efficient and stable electrocatalysts.

4.3. Nanotubes

In 2018, Zanoni et al. modified Ti/TiO_2 nanotubes (Ti/TiO_2NT) via a layer-by-layer route. ZIF-8 NPs with ca. 50 nm in size were coated on Ti/TiO_2NT.[75] FTIR analysis indicated that the host-guest interaction depended greatly on the pore structure and the chemical properties of linkers in MOFs. On Ti/TiO_2NT-ZIF-8 electrode, CO_2 can be photoelectrically converted into methanol and ethanol fuel under UV irradiation at room temperature. The as-prepared Zn-MOF not only acts adsorbent on CO_2 adsorption/activation, but also acts as a cocatalyst to transfer excited electrons for photocatalytic reduction.

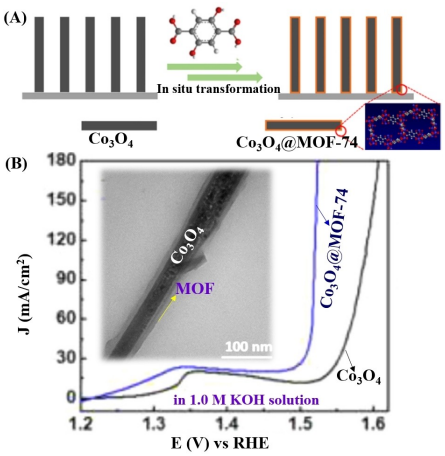

Figure 15. (A) Schematic illustration for the in-situ coating of MOF-74 onto Co_3O_4 nanowires, (B) Comparison of polarization curves between bare Co_3O_4 and MOF-coated Co_3O_4. Adopted with permission from Elsevier.[74]

4.4. Nanosheets

Compared with traditional MOF bulk crystals, ultra-thin MOF nanosheets have excellent properties in enantioselective sensing, chiral separation and asymmetric catalysis. Taking advantage of their good mass diffusion advantages, superior flexibility and enhanced interaction with the incoming substrate can be achieved.[76] For example, Sun et al. first developed and used ultra-thin two-dimensional zinc porphyrin based Zn-MOF nanosheet to reduce CO_2 to CO,[77] so as to establish two novel non-noble metal hybrid photocatalytic systems. The catalyst exhibited excellent photocatalytic activity and selectivity under mild reaction conditions. The electrochemical impedance and PL spectrum tests indicated that the Zn-MOF nanosheet surpassed Zn-MOF bulk with better charge transfer ability and longer lifetime of photogenerated electron-hole pairs, which finally led to boosted photocatalytic efficiency and selectivity.

4.5. Hollow nanostructures

Due to the characteristics of low density, large surface area, high bearing capacity and material economy, hollow nanostructures have attracted extensive attention. Combined with the inherent characteristics of MOFs, hollow MOFs can act as a new platform for exploring catalytic applications.[78] Nevertheless, compared with the preparation of various hollow inorganic nanomaterials, the construction of hollow MOFs is still a great challenge, of which few relevant works were reported.[79] the traditional template restriction strategy has some inherent limitations.[80] Until recently, the Wang's group designed a new method based on heterogeneous MOFs containing two metals, so that the hollow MOFs can be easily realized by the simple solvothermal reaction.

Well-Defined Zn/Ni-MOF-2 hollow cubes were obtained due to the nanoscale Kirkendall effect (Figure 16). Specifically, using 1,4-phthalic acid (H_2BDC) as organic ligand, $Zn^{2+}$and Ni^{2+} as metal nodes, and N, N-Dimethylacetamide (DMAC)/ethanol as mixed solvents,[81] Hollow Zn/Ni-MOF-2 was obtained after simple solvothermal treatment. Besides, it is worth noting that the molar ratio of Zn/Ni was decreased, which is typical due to Kirkendall effect. In particular, Zn^{2+} was enriched in the initially formed nano-cube, and then the content of Ni^{2+} increased gradually. With the transformation of morphology from nano-cube to nano-shell, the crystal structure of Zn/Ni-MOF-5 was also changed to Zn/Ni-MOF-2, and cavities were formed in the Zn/Ni MOF nano-cube. Importantly, through similar methods based on heterogeneous metal systems, a series of clearly-defined MOFs with the hollow structure are synthesized. For example, Figure 16C presented the formation process for Fe^{III}-ICP hollow structure.

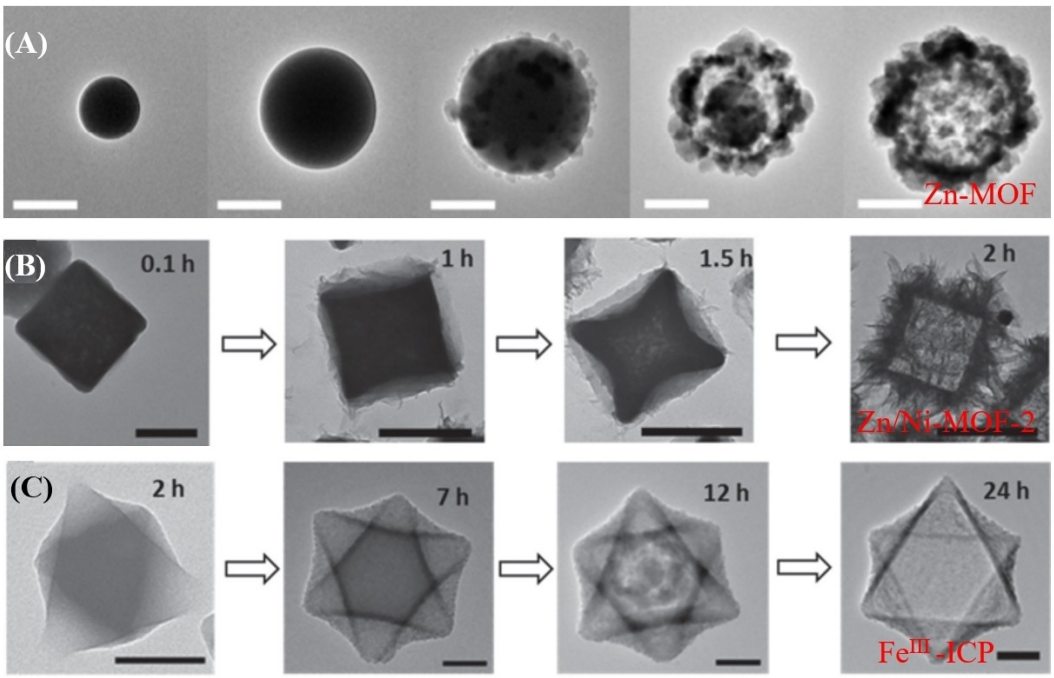

Figure 16. TEM images of (A) Zn-MOF, (B) Zn/Ni-MOF-2 and (C) Fe^{III}-ICP obtained at different reaction times. Reproduced with permission from WILEY.[81]

4.6. Microcapsules

Microcapsules are a kind of special hollow structural materials, which have the characteristics of low density, high specific surface area and easy to accommodate guest molecules. Most of the reported microcapsules/nanocapsules are totally closed structures that only expose the outer surface, resulting in the contact with the reaction substrate only the outer surface of the capsule, and the inner surface of the shell can not be fully utilized. The inner and outer shell with open structure can both participate in the catalytic reaction, which is more conducive to mass diffusion, and has potential application value in the field of catalysis. Especially for photocatalysis, the inner and outer parts of the open structure can contact both the substrate and light, leading to the shortened transmission distance of photo-generated charge carriers and more quick participation in the reaction.

Recently, some scholars began to pay attention to the preparation of open structure microcapsules/nanocapsules using MOFs. For example (Figure 17), Wang et al. introduced polyacid anions into the synthesis process of MOFs to form a competitive relationship between polyacid anions and organic ligands, and then coordinated with metal clusters to prepare bowl-shaped MOFs microcapsule (MBM).[82] Maji et al. prepared Zn (OPE)·2H_2O nano vehicles and toroids by controlling reaction parameters, using oligophenylene acetylene dicarboxylic acid (OPEA) as linker to coordinate with $Zn(OAC)_2$ via directed self-assembly strategy.[83] The as-prepared MOF is dynamic and soft, which has efficient daylighting applications.

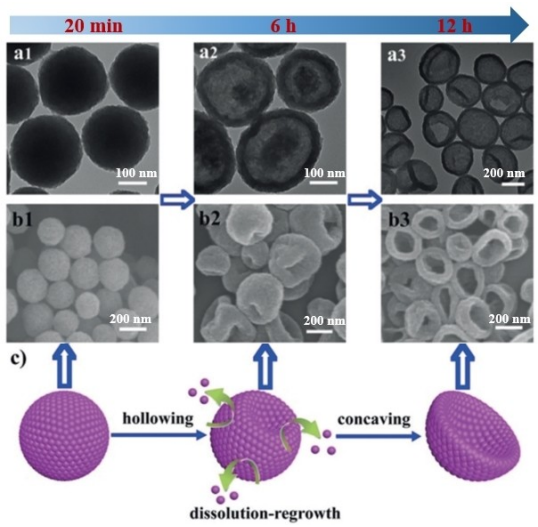

Figure 17. a) TEM and b) SEM images of MBM obtained at prolonged reaction time, c) Proposed formation process for MBM. Reproduced with permission from WILEY.[82]

4.7. Hierarchical nanostructures

Recently, hierarchical nanostructures have become a research hotspot in materials, chemistry, catalysis, biomedicine and related interdisciplinary fields, due to their unique physical-chemical properties, including controllable hierarchical structure, large surface area, open porous structure, excellent surface properties, and etc.[84] For example, Zhang et al. synthesized a foam-like trimetallic MOFs [$(Ni_2Co_1)_{1-x}Fe_x$-MOF-NF] at room

temperature, which displayed good activity and excellent stability in the electrocatalytic evolution of oxygen.[85] The quick mixing of Fe, Co and Ni precursor solutions will lead to the formation of such porous three-dimensional hierarchical structure (Figure 18A).

In addition, hierarchical Ru-MOF nanoflowers were fabricated (Figure 18B), which can be applied as photocatalyst for visible-light-driven reduction of CO_2.[86] The production rate of $HCOO^-$ can reach as high as 77.2 $\mu mol\,g^{-1}\,h^{-1}$ when using triethanolamine (TEOA) as hole scavenger. Moreover, the photocatalytic performance by Ru-MOF with different sizes was compared, and the results were shown in Figure 19C. It can be observed that the unique flower-like nanostructure significantly improves the photocatalytic activity for $HCOO^-$ production. After 8 h irradiation, the yield of $HCOO^-$ by nanoflowers was about 2.5 times that by solid microcrystals. In addition, the unique nanostructure also significantly improves the stability and recyclability of Ru-MOF.

5. Multivariate MOFs (MTV MOFs)

Recently, it has been reported the design and synthesis of multivariate MOFs (MTV MOFs) were used as heterogeneous catalysts.[87–89] The MTV refers to the introduction of multiple or mixed organic functional groups into the existing framework. The MTV-MOFs have basic properties that specific functionalities are occupied a similar place in the framework and the amount of each functionality can be adjusted. Multiple organic linkers with distinct lengths were used in MTV MOFs, where they were located in different clusters/nodes in the framework, to achieve a high degree of MTV crystalline porous structure. For example, the existing energy limit of visible light photocatalysis can be broken through multi-photon photochemical processes. Duan et al. reported that novel two-photon responsive ligands (bis(3,5-**dicarboxyphenyl)pyridine and bis(3,5-dicarboxyphenyl)-methylpyridinium) could be introduced** into a single MOFs (ZJU-56) through a MTV strategy. The as-prepraed MOFs were used for photocatalytic C–N and C–C oxidative coupling reactions. Through the intensity-dependent experiments, it was proved that MTV MOFs containing high-

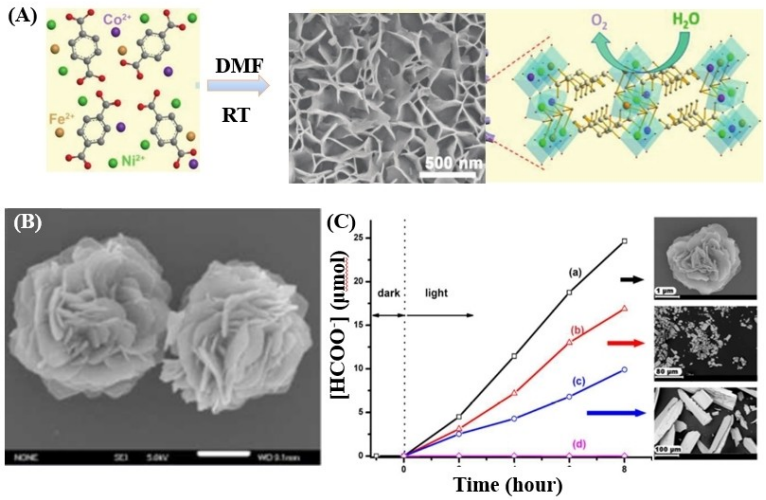

Figure 18. (A) Illustration of the preparation of porous three-dimensional hierarchical $(Ni_2Co_1)_{1-x}Fe_x$-MOF-NF, (B) SEM image of flower shaped Ru-MOF, (C) Photocatalytic production of $HCOO^-$ by Ru-MOF with different shapes. Reproduced with permission from WILEY and Royal Society of Chemistry [85,86]

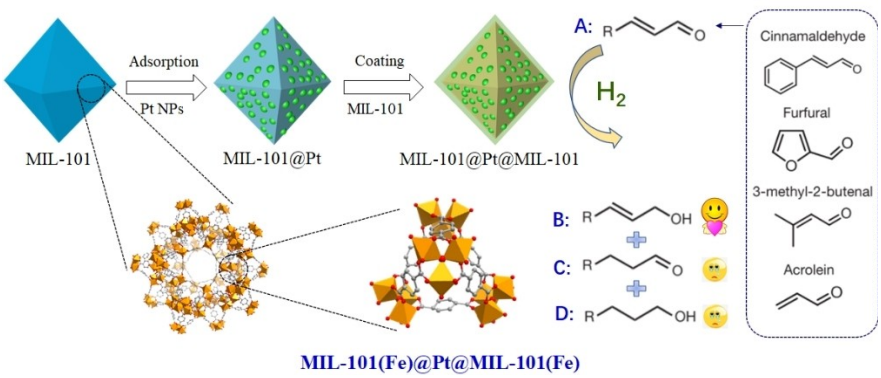

Figure 19. Synthetic route for the preparation of sandwich MIL-101@Pt@MIL-101, and its application for selective hydrogenation of unsaturated aldehydes.

density and ordered photoactive motifs could enhance the photocatalytic efficiency via a two-photon absorption process.[87]

6. Multi-Strategy with synergistic regulation

6.1. MOFs@NPs@MOFs

The coordinatively-unsaturated metal sites (CUSs) in MOFs can be easily adjusted to realize the interaction with reactants. To activate the target chemical bond in the reactant and reduce the energy barrier of the required reaction, Tang et al. used MIL-101@Pt@MIL-101 sandwich structure as a hydrogenation catalyst to explore this concept.[7] The multicomponent composite consisted of a layer of Pt NPs wrapped between the MIL-101 core and MIL-101 shell (Figure 19). Herein, the core-shell contains Fe^{3+} or Cr^{3+} trimers, which was connected with 1,4-benzoic acid ester (BDC) connector. The study found that the optimized MIL-101(Fe)@Pt@MIL-101(Fe) can efficiently and stably catalyze a series of α,β-unsaturated aldehydes and significantly improve the selectivity for the production of unsaturated alcohols. The preferential interaction between MOF metal sites in MOFs and C=O group (rather than C=C group), were calculated to make the hydrogenation of embedded Pt NPs a thermodynamically favorable reaction. Overall, the results of this study confirm the great potential of sandwich-type MOFs as a novel catalytic carrier.[90,91] This has proven to be an effective way to respond to important but challenging reactions.

6.2. MOFs@NPs@COFs

Sandwich type MOFs@NPs@COFs was also fabricated.[92] Due to the great potential of NH_2-MIL-125(Ti) (denoted as Ti-MOF) in photocatalysis, it was selected as the core, with the covering of hydrophobic COFs shell. Pt NPs were limited between the core and shell (Figure 20). Herein, Pt NPs can promote efficient charge separation in the LUMO-HOMO of Ti-MOFs, resulting the formation of electron-rich Pt NPs. Besides, due to hydrophobic and highly porous COFs shell, the reactants were easily enriched around Pt NPs, and the diffusion was also are greatly promoted. The limited interfacial pores can act as nano-reactors, which will ensure the rapid electron transfer and mass diffusion between Pt NPs and substrates. Thus, the as-prepared Ti-MOF@Pt@COF displayed charming photocatalytic activity for styrene hydrogenation. Under 40 min irradiation by visible light, the conversion of styrene reached ca. 100% by Ti-MOF@Pt@COF (Figure 20A). Whereas, the value was 72% and 51% for Ti-MOF@Pt (Figure 20B) and Ti-MOF@COF/Pt, respectively. Although some countable MOFs/COFs composites have been reported previously, this is the first work of sandwich MOFs@NPs@COFs for photocatalysis. This interfacial confinement strategy provides a new way for the rational design of various MOF-based materials to achieve high efficiency in heterogeneous catalysis.

6.3. MOFs@MOFs@Polymer

The early studies on the grafting of polymer onto MOFs often lead to the blockage of MOF particles and the reduction of specific surface area. In order to overcome this problem, McDonald et al. designed a polyMOF material with a core-shell structure.[93] The shell can not only provide reaction sites for polymer growth, but also prevent pore blockage. As displayed in Figure 21, with MOF-5 as the core and IRMOF-3 as the shell,

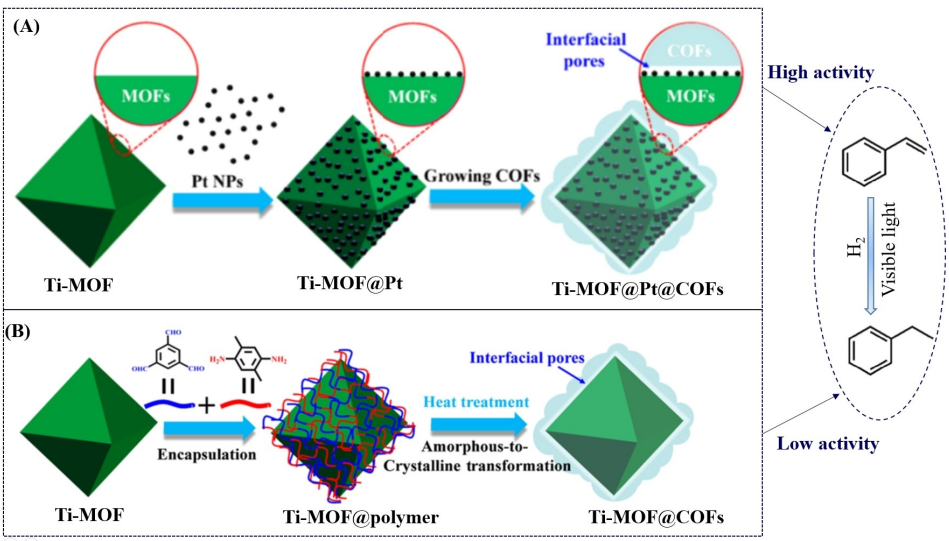

Figure 20. Diagrammatic sketch for the preparation of (A)Ti-MOF@Pt@COFs and (B) Ti-MOF@COFs, as well as corresponding activity for the hydrogenation of styrene. Adapted with permission from ACS.[92]

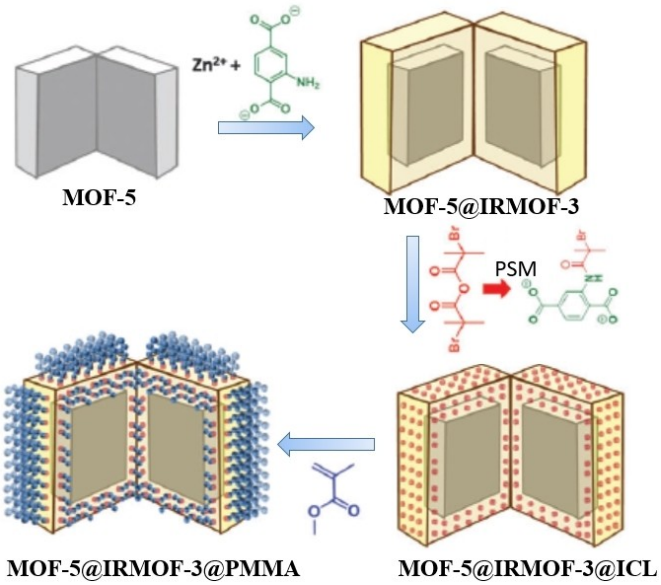

Figure 21. Diagrammatic sketch for the preparation of MOF-5@IRMOF-3@PMMA. Adapted with permission from RSC.[93]

IRMOF-3 containing 2-aminoterephthalate linker can be grown on the surface of MOF-5. Subsequently, the initiator was installed on the shell of IRMOF-3 by the selective reaction of the amine group on IRMOF-3 with 2-bromoisobutyric anhydride. Finally, polymethylmethacrylate (PMMA) was formed by polymerization of monomers under the action of initiator. Since the initiator is only located on the shell, the polymerization reaction is limited to the shell of the crystal, and the MOF-5 core is intact. The surface area of MOFs grafted with PMMA was more than 2800 m^2/g, which was only 15% lower than that of MOFs functionalized with initiator. This shows that the core-shell structure can effectively reduce the pore blockage caused by grafting technology, which provides novel idea for the preparation of polyer@MOFs composite with high porosity.

6.4. Fe_3O_4@enzyme@MOFs

Recently, amidase was successfully immobilized into porous MOFs for efficient biocatalysis.[94] As shown in Figure 22A, core-shell magnetic hierarchically porous Fe_3O_4@MOF was prepared and employed as support for immobilizing amidase. Different kinds of MOFs were tested, such as $Cu_3(BTC)_2$, ZIF-8, MIL-100(Fe), UiO-66-NH_2 and hierarchical UiO-66-NH_2. Among these, hierarchical UiO-66-NH_2 was the best one for amidase immobilization. The corresponding yield for amidase immobilization and recovery was 92.2% and 88.2%, respectively. Besides, the immobilized amidase displayed significantly enhanced stability toward high temperature and organic solvent (Figure 22B–C). In the test of cyclic runs, the activity of amidase was maintained at 98.2% after 15 cycles. Long time stability was also observed for the preparation of (S)-4-fluorophenylglycine. After 20 days of reaction, only 26% activity remained for free amidase. Whereas, the value greatly increased to ca. 86% for immobilized amidase, indicating the vital role of porous MOFs. This work opens up a new field. The preparation methods of various functional magnetic MOFs have gradient porosity, which broadens the application prospect of enzymes and stimulates the immobilization of layered porous magnetic MOFs with certain structures.

7. Summary and outlook

After more than 20 years of active research, the unremitting efforts committed to MOFs-based catalysts have formed a rich database. In this review, we have summarized the strategies for

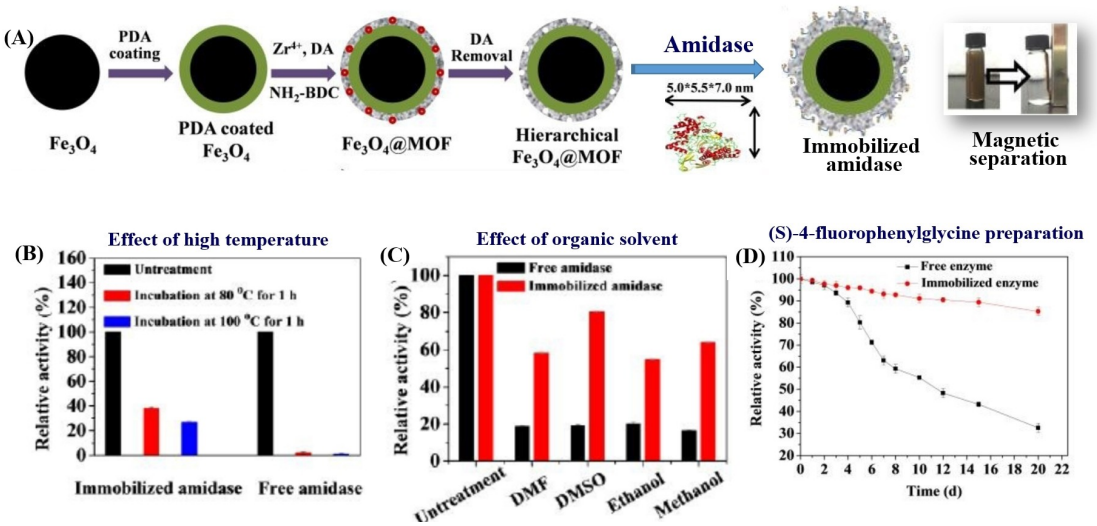

Figure 22. (A) Schematic illustration for the fabrication of hierarchical Fe_3O_4@MOF and immobilization of amidase, as well as photo image for magnetic separation. (B) Effect of high temperature and (C) organic solvent on the tolerance of amidase before and after immobilization. (D) The long time stability for the preparation of (S)-4-fluorophenylglycine under different conditions. Adapted with permission from RSC.[94]

nanospace engineering of MOFs for heterogeneous catalysis. Reasonable design and adjustment mainly focus on three parts: pores, guest species and surface modifiers. Thanks to abundant organic units and diverse topologies, more and more new MOFs with high performance have been successfully synthesized and applied in the field of catalysis. It is expected that MOFs may replace the traditional homogeneous catalysts in the field of the fine chemical industry. Meanwhile, it can also be predicted that MOFs can enable the chemical reaction to proceed under mild and green reaction conditions, so as to achieve sustainable development.

Although the prospect is bright, facing the opportunities, the fabrication and practical application of MOFs in the future still faces many challenges:

(1) The diversity of catalysts is the premise for the wide application of catalysts. The most important thing is to develop MOFs and MOFs-based composites with functional diversity. It is necessary to develop various loading modes to prepare new MOFs with diverse morphology, good crystallization performance, high stability, good economy and strong functionality.
(2) The regulation of MOFs pore size is limited to the empirical stage, it is still difficult to accurately control the size and shape of MOFs while maintaining structural integrity. The regulation mechanism needs to be deeply studied to achieve accurate control, especially the accurate control of reaction kinetics and thermodynamic pore size distribution.
(3) Although the manufacturing of yolk-shell reactor has solved the problem of poor diffusion of reactants to the catalyst core, it is still necessary to avoid the use of hard templates or develop more sacrificial templates.
(4) Nano-MOFs have been demonstrated to be good candidates as catalysts in various fields. However, large-scale application is hindered due to its complicated preparation steps and low yields. It is urgent to develop more simple and practical ways for nano-MOFs fabrication.
(5) For electrocatalysis, MOFs were frequently calcined to improve conductivity and catalytic performance, but it also leads to the destruction of ordered pore structure and the sharp decrease of specific surface area. To avoid this limitation, it is better to introduce highly conductive components or develop two-dimensional conductive MOFs.
(6) At present, in some simple model reactions, great progress has been achieved in heterogeneous catalysis by MOFs. However, for more challenging organic reactions in traditional homogeneous systems, there is still a huge distance for MOFs system. MOFs need to be further well-designed for synthesizing high value-added chemicals.
(7) The common characterization method of MOFs is based on non-in-situ method, which cannot well monitor its reaction kinetics under working conditions. For deeper study on catalytic mechanism, more investigations need to be performed via capturing the transition state.

In summary, the research on MOF catalysis is still in its infancy. We believe that we have room for development to meet the existing challenges. What we have collected here is an overview of the strategies for nanospace engineering of MOFs for heterogeneous catalysis. The nanospace engineering may only be the tip of the technology. There are more exciting discoveries waiting for us to discover and explore. We hope that this review can stimulate new insights and provide guidance for future research in related and cross fields.

Acknowledgements

The authors are grateful for the financial support of the National Natural Science Foundation of China (21876154), Zhejiang Provincial Natural Science Foundation China (LR18B070001), and partially supported by the Robert A. Welch Foundation (B-0027) and the US National Science Foundation (ECCS- 2029800) (SM).

Conflict of Interest

The authors declare no conflict of interest.

Keywords: Metal-Organic Framework · Nanospace Engineering · Pore · Host-Guest · Heterogeneous Catalysis

[1] O. Yaghi, H. Li, *J. Am. Chem. Soc.* **1995**, *117*, 10401–10402.
[2] J. Lee, O. K. Farha, J. Roberts, K. A. Scheidt, S. T. Nguyen, J. T. Hupp, *Chem. Soc. Rev.* **2009**, *38*, 1450–1459.
[3] L. Zhu, X.-Q. Liu, H.-L. Jiang, L.-B. Sun, *Chem. Rev.* **2017**, *117*, 8129–8176.
[4] A. Bavykina, N. Kolobov, I. S. Khan, J. A. Bau, A. Ramirez, J. Gascon, *Chem. Rev.* **2020**, *120*, 8468–8535.
[5] J. Liang, Z. Liang, R. Zou, Y. Zhao, *Adv. Mater.* **2017**, *29*, 1701139.
[6] L. Jiao, Y. Wang, H. L. Jiang, Q. Xu, *Adv. Mater.* **2018**, *30*, 1703663.
[7] M. Zhao, K. Yuan, Y. Wang, G. Li, J. Guo, L. Gu, W. Hu, H. Zhao, Z. Tang, *Nature.* **2016**, *539*, 76–80.
[8] D. Li, H. Q. Xu, L. Jiao, H. L. Jiang, *EnergyChem.* **2019**, *1*, 100005.
[9] X. Li, X. Yang, H. Xue, H. Pang, Q. Xu, *EnergyChem.* **2020**, *2*, 100027.
[10] L. Chen, Q. Xu, *Matter.* **2019**, *1*, 57–89.
[11] O. K. Farha, I. Eryazici, N. C. Jeong, B. G. Hauser, C. E. Wilmer, A. A. Sarjeant, R. Q. Snurr, S. T. Nguyen, A. O. z. r. Yazaydın, J. T. Hupp, *J. Am. Chem. Soc.* **2012**, *134*, 15016–15021.
[12] J. Lan, Y. Qu, X. Zhang, H. Ma, P. Xu, J. Sun, *J. CO_2 Util.* **2020**, *35*, 216–224.
[13] J. Pang, Z. Di, J. S. Qin, S. Yuan, C. T. Lollar, J. Li, P. Zhang, M. Wu, D. Yuan, M. Hong, H.-C. Zhou, *J. Am. Chem. Soc.* **2020**, *142*, 15020–15026.
[14] S. Wu, X. Xing, D. Wang, J. Zhang, J. Chu, C. Yu, Z. Wei, M. Hu, X. Zhang, Z. Li, *ACS Sustainable Chem. Eng.* **2019**, *8*, 148–153.
[15] O. M. Yaghi, M. O'Keeffe, N. W. Ockwig, H. K. Chae, M. Eddaoudi, J. Kim, *Nature.* **2003**, *423*, 705–714.
[16] C. Gomes Silva, I. Luz, F. X. Llabres i Xamena, A. Corma, H. García, *Chem. Eur. J.* **2010**, *16*, 11133–11138.
[17] E. Haque, J. H. Jeong, S. H. Jhung, *CrystEngComm.* **2010**, *12*, 2749–2754.
[18] G. Férey, *Chem. Soc. Rev.* **2008**, *37*, 191–214.
[19] D. Liu, D. Zou, H. Zhu, J. Zhang, *Small.* **2018**, *14*, 1801454.
[20] N. A. Khan, Z. Hasan, S. H. Jhung, *Coord. Chem. Rev.* **2018**, 376, 20–45.
[21] Z. Yin, S. Wan, J. Yang, M. Kurmoo, M.-H. Zeng, *Coord. Chem. Rev.* **2019**, *378*, 500–512.
[22] R. Dalapati, S. Biswas, *Sens. Actuators B* **2017**, *239*, 759–767.
[23] R. Xu, Z. Wang, M. Wang, Z. Qiao, J. Wang, *J. Membr. Sci.* **2019**, *573*, 455–464.
[24] V. Guillerm, T. Grancha, I. Imaz, J. Juanhuix, D. Maspoch, *J. Am. Chem. Soc.* **2018**, *140*, 10153–10157.
[25] Y. Zhang, B. Gui, R. Chen, G. Hu, Y. Meng, D. Yuan, M. Zeller, C. Wang, *Inorg. Chem.* **2018**, *57*, 2288–2295.
[26] B. Li, D. Ma, Y. Li, Y. Zhang, G. Li, Z. Shi, S. Feng, M. J. Zaworotko, S. Ma, *Chem. Mater.* **2016**, *28*, 4781–4786.

[27] S.-T. Zheng, J. T. Bu, Y. Li, T. Wu, F. Zuo, P. Feng, X. Bu, *J. Am. Chem. Soc.* **2010**, *132*, 17062–17064.
[28] Q. Yao, J. Su, O. Cheung, Q. Liu, N. Hedin, X. Zou, *J. Mater. Chem.* **2012**, *22*, 10345–10351.
[29] G. C. Shearer, S. Chavan, S. Bordiga, S. Svelle, U. Olsbye, K. P. Lillerud, *Chem. Mater.* **2016**, *28*, 3749–3761.
[30] L. G. Qiu, T. Xu, Z. Q. Li, W. Wang, Y. Wu, X. Jiang, X. Y. Tian, L. D. Zhang, *Angew. Chem. Int. Ed.* **2008**, *47*, 9487–9491; *Angew. Chem.* **2008**, *120*, 9629–9633.
[31] K. Shen, L. Zhang, X. Chen, L. Liu, D. Zhang, Y. Han, J. Chen, J. Long, R. Luque, Y. Li, *Science.* **2018**, *359*, 206–210.
[32] C. Guo, Y. Zhang, Y. Guo, L. Zhang, Y. Zhang, J. Wang, *Chem. Commun.* **2018**, *54*, 252–255.
[33] Q. Yang, Q. Xu, H.-L. Jiang, *Chem. Soc. Rev.* **2017**, *46*, 4774–4808.
[34] G. Zhan, H. C. Zeng, *Nanopart. Catal.: Adv. Synth. Appl.* **2021**, 183–214.
[35] P. Hu, J. V. Morabito, C.-K. Tsung, *ACS Catal.* **2014**, *4*, 4409–4419.
[36] Y. Luan, Y. Qi, H. Gao, N. Zheng, G. Wang, *J. Mater. Chem. A.* **2014**, *2*, 20588–20596.
[37] G. Lu, S. Li, Z. Guo, O. K. Farha, B. G. Hauser, X. Qi, Y. Wang, X. Wang, S. Han, X. Liu, J. S. DuChene, H. Zhang, Q. Zhang, X. Chen, J. Ma, S. C. J. Loo, W. D. Wei, Y. Yang, J. T. Hupp, F. Huo, *Nat. Chem.* **2012**, *4*, 310–316.
[38] A. Aijaz, A. Karkamkar, Y. J. Choi, N. Tsumori, E. Rönnebro, T. Autrey, H. Shioyama, Q. Xu, *J. Am. Chem. Soc.* **2012**, *134*, 13926–13929.
[39] C. Wang, H. Zhang, C. Feng, S. Gao, N. Shang, Z. Wang, *Catal. Commun.* **2015**, *72*, 29–32.
[40] H.-L. Jiang, T. Akita, T. Ishida, M. Haruta, Q. Xu, *J. Am. Chem. Soc.* **2011**, *133*, 1304–1306.
[41] Y. Qin, X. Han, Y. Li, A. Han, W. Liu, H. Xu, J. Liu, *ACS Catal.* **2020**, *10*, 5973–5978.
[42] C.-H. Kuo, Y. Tang, L.-Y. Chou, B. T. Sneed, C. N. Brodsky, Z. Zhao, C.-K. Tsung, *J. Am. Chem. Soc.* **2012**, *134*, 14345–14348.
[43] Y. Liu, W. Zhang, S. Li, C. Cui, J. Wu, H. Chen, F. Huo, *Chem. Mater.* **2014**, *26*, 1119–1125.
[44] L. Luo, W.-S. Lo, X. Si, H. Li, Y. Wu, Y. An, Q. Zhu, L.-Y. Chou, T. Li, C.-K. Tsung, *J. Am. Chem. Soc.* **2019**, *141*, 20365–20370.
[45] J. Teng, M. Chen, Y. Xie, D. Wang, J.-J. Jiang, G. Li, H.-P. Wang, Y. Fan, Z.-W. Wei, C.-Y. Su, *Chem. Mater.* **2018**, *30*, 6458–6468.
[46] Q. Dang, H. Huang, L. Li, X. Lyu, S. Zhong, Y. Yu, D. Xu, *Chem. Mater.* **2021**, *33*, 5690–5699.
[47] S. Wang, Y. Fan, J. Teng, Y. Z. Fan, J. J. Jiang, H. P. Wang, H. Grützmacher, D. Wang, C. Y. Su, *Small.* **2016**, *12*, 5702–5709.
[48] R. P. Ye, X. Wang, C. A. H. Price, X. Liu, Q. Yang, M. Jaroniec, J. Liu, *Small.* **2021**, *17*, 1906250.
[49] T. Zeng, X. Zhang, S. Wang, H. Niu, Y. Cai, *Environ. Sci. Technol.* **2015**, *49*, 2350–2357.
[50] C.-F. Zhang, L.-G. Qiu, F. Ke, Y.-J. Zhu, Y.-P. Yuan, G.-S. Xu, X. Jiang, *J. Mater. Chem. A.* **2013**, *1*, 14329–14334.
[51] C. Inman, J. M. Knaust, S. W. Keller, *Chem. Commun.* **2002**, 156–157.
[52] G. Férey, C. Mellot-Draznieks, C. Serre, F. Millange, J. Dutour, S. Surblé, I. Margiolaki, *Science.* **2005**, *309*, 2040–2042.
[53] J. Song, Z. Luo, D. K. Britt, H. Furukawa, O. M. Yaghi, K. I. Hardcastle, C. L. Hill, *J. Am. Chem. Soc.* **2011**, *133*, 16839–16846.
[54] J.-S. Qin, D.-Y. Du, W. Guan, X.-J. Bo, Y.-F. Li, L.-P. Guo, Z.-M. Su, Y.-Y. Wang, Y.-Q. Lan, H.-C. Zhou, *J. Am. Chem. Soc.* **2015**, *137*, 7169–7177.
[55] S. Mukhopadhyay, J. Debgupta, C. Singh, A. Kar, S. K. Das, *Angew. Chem. Int. Ed.* **2018**, *130*, 1936–1941.
[56] B. P. Biswal, D. B. Shinde, V. K. Pillai, R. Banerjee, *Nanoscale.* **2013**, *5*, 10556–10561.
[57] M. S. Alivand, N. H. M. H. Tehrani, M. Askarieh, E. Ghasemy, M. D. Esrafili, R. Ahmadi, H. Anisi, O. Tavakoli, A. Rashidi, *J. Hazard. Mater.* **2021**, *416*, 125973.
[58] D. Wei, W. Tang, Y. Gan, X. Xu, *Catal. Sci. Technol.* **2020**, *10*, 5666–5676.
[59] A. Dhakshinamoorthy, A. M. Asiri, H. Garcia, *Dalton T.* **2020**, *49*, 11059–11072.
[60] Y. Hu, L. Dai, D. Liu, W. Du, Y. Wang, *Renewable Sustainable Energy Rev.* **2018**, *91*, 793–801.
[61] H. An, M. Li, J. Gao, Z. Zhang, S. Ma, Y. Chen, *Coord. Chem. Rev.* **2019**, *384*, 90–106.
[62] S. Dutta, N. Kumari, S. Dubbu, S. W. Jang, A. Kumar, H. Ohtsu, J. Kim, S. H. Cho, M. Kawano, I. S. Lee, *Angew. Chem. Int. Ed.* **2020**, *132*, 3444–3450.
[63] B. Le Ouay, T. Uemura, *Israel, J. Chem.* **2018**, *58*, 995–1009.
[64] T. Kong, G. Guo, J. Pan, L. Gao, Y. Huo, *Dalton T.* **2016**, *45*, 18084–18088.
[65] M. Ding, H.-L. Jiang, *ACS Catal.* **2018**, *8*, 3194–3201.
[66] L. Feng, Y. Wang, S. Yuan, K. Y. Wang, J. L. Li, G. S. Day, D. Qiu, L. Cheng, W.-M. Chen, S. T. Madrahimov, *ACS Catal.* **2019**, *9*, 5111–5118.
[67] G. Y. Qiao, S. Yuan, J. Pang, H. Rao, C. T. Lollar, D. Dang, J. S. Qin, H. C. Zhou, J. Yu, *Angew. Chem. Int. Ed.* **2020**, *59*, 18224–18228; *Angew. Chem.* **2020**, *132*, 18381–18385.
[68] N. Stock, S. Biswas, *Chem. Rev.* **2012**, *112*, 933–969.
[69] J. Zhao, X. Liu, Y. Wu, D.-S. Li, Q. Zhang, *Coord. Chem. Rev.* **2019**, *391*, 30–43.
[70] W. Liu, R. Yin, X. Xu, L. Zhang, W. Shi, X. Cao, *Adv. Sci.* **2019**, *6*, 1802373.
[71] X. Xiao, L. Zou, H. Pang, Q. Xu, *Chem. Soc. Rev.* **2020**, *49*, 301–331.
[72] S. Vaucher, M. Li, S. Mann, *Angew. Chem. Int. Ed.* **2000**, *39*, 1793–1796; *Angew. Chem.* **2000**, *112*, 1863–1866.
[73] K. Xie, Q. Fu, Y. He, J. Kim, S. J. Goh, E. Nam, G. Qiao, P. Webley, *Chem. Commun.* **2015**, *51*, 15566–15569.
[74] W. Gao, W. Gou, R. Wei, X. Bu, Y. Ma, J. C. Ho, *Appl. Mater. Res.* **2020**, *21*, 100820.
[75] J. Cardoso, S. Stulp, J. De Brito, J. Flor, R. Frem, M. Zanoni, *Appl. Catal. B* **2018**, *225*, 563–573.
[76] C. Tan, K. Yang, J. Dong, Y. Liu, Y. Liu, J. Jiang, Y. Cui, *J. Am. Chem. Soc.* **2019**, *141*, 17685–17695.
[77] L. Ye, Y. Gao, S. Cao, H. Chen, Y. Yao, J. Hou, L. Sun, *Appl. Catal. B* **2018**, *227*, 54–60.
[78] Z. Zhang, Y. Chen, S. He, J. Zhang, X. Xu, Y. Yang, F. Nosheen, F. Saleem, W. He, X. Wang, *Angew. Chem. Int. Ed.* **2014**, *53*, 12517–12521; *Angew. Chem.* **2014**, *126*, 12725–12729.
[79] H. Kim, M. S. Lah, *Dalton Trans.* **2017**, *46*, 6146–6158.
[80] I. Lee, S. Choi, H. J. Lee, M. Oh, *Cryst. Growth Des.* **2015**, *15*, 5169–5173.
[81] X. Xu, Z. Zhang, X. Wang, *Adv. Mater.* **2015**, *27*, 5365–5371.
[82] T. He, X. Xu, B. Ni, H. Lin, C. Li, W. Hu, X. Wang, *Angew. Chem. Int. Ed.* **2018**, *57*, 10148–10152; *Angew. Chem.* **2018**, *130*, 10305–10309.
[83] V. M. Suresh, S. J. George, T. K. Maji, *Adv. Funct. Mater.* **2013**, *23*, 5585–5590.
[84] H. Yang, X. Song, T. Yang, Z. Liang, C. Fan, X. Hao, *RSC Adv.* **2014**, *4*, 15720–15726.
[85] Q. Qian, Y. Li, Y. Liu, L. Yu, G. Zhang, *Adv. Mater.* **2019**, *31*, 1901139.
[86] S. Zhang, L. Li, S. Zhao, Z. Sun, M. Hong, J. Luo, *J. Mater. Chem. A.* **2015**, *3*, 15764–15768.
[87] H. Li, Y. Yang, C. He, L. Zeng, C. Duan, *ACS Catal.* **2018**, *9*, 422–430.
[88] Q. Xia, Z. Li, C. Tan, Y. Liu, W. Gong, Y. Cui, *J. Am. Chem. Soc.* **2017**, *139*, 8259–8266.
[89] S. Patial, P. Raizada, V. Hasija, P. Singh, V. K. Thakur, V.-H. Nguyen, *Mater. Today Energ.* **2020**, 100589.
[90] Q. Yang, W. Liu, B. Wang, W. Zhang, X. Zeng, C. Zhang, Y. Qin, X. Sun, T. Wu, J. Liu, *Nat. Commun.* **2017**, *8*, 1–9.
[91] Z. Xu, W. Zhang, J. Weng, W. Huang, D. Tian, F. Huo, *Nano Res.* **2016**, *9*, 158–164.
[92] D. Sun, D.-P. Kim, *ACS Appl. Mater. Interfaces* **2020**, *12*, 20589–20595.
[93] K. A. McDonald, J. I. Feldblyum, K. Koh, A. G. Wong-Foy, A. J. Matzger, *Chem. Commun.* **2015**, *51*, 11994–11996.
[94] C. Lin, K. Xu, R. Zheng, Y. Zheng, *Chem. Commun.* **2019**, *55*, 5697–5700.

Manuscript received: October 3, 2021
Revised manuscript received: November 22, 2021
Accepted manuscript online: November 22, 2021
Version of record online: December 1, 2021